Chapter 8

MICROWAVE COMPONENTS AND CIRCUITS

We have discussed in the previous chapter some of the high-frequency effects which occur in grid-controlled tubes. Lead inductances, interelectrode capacitances, conductor resistances, beam loading, and electron transit-time effects contribute deleteriously to the performance of high-frequency, grid-controlled amplifiers. As will be noted later in this chapter, conductor resistance losses actually worsen with increasing frequency due to an effect known as "skin effect." Furthermore, as frequency increases, it is possible for lead wires to have lengths comparable with a wavelength, in which case they can act as antennas and radiate electromagnetic energy. These considerations lead one to abandon the wires and lumped components used at lower frequencies and to seek new and more appropriate components for microwave frequencies.

Let us first consider the evolution of the tuned circuit as the resonant frequency is increased into the microwave range. At low and moderate frequencies, lumped-constant resonant circuits, such as the one illustrated schematically in Figure 8-1(a), are frequently used in electronic circuitry. The resonant frequency is given by $f = 1/2\pi\sqrt{LC}$, where L is the inductance, and C is the capacitance. In a tetrode amplifier circuit, for example, an inductance L may be used to resonate with the interelectrode and stray capacitances of the output circuit so as to give maximum gain at a particular frequency.

As the operating frequency is increased, both the capacitance and inductance could be decreased in order to maintain resonance at the operating frequency. However, for the case of the tetrode amplifier, a limiting value of the capacitance is soon reached for two practical reasons. First, transit-time effects set a limit to how far the electrodes can be pulled apart. Second, the area to which the beam cross section can be reduced may be limited by (1) the maximum allowable cathode current density or (2) considerations

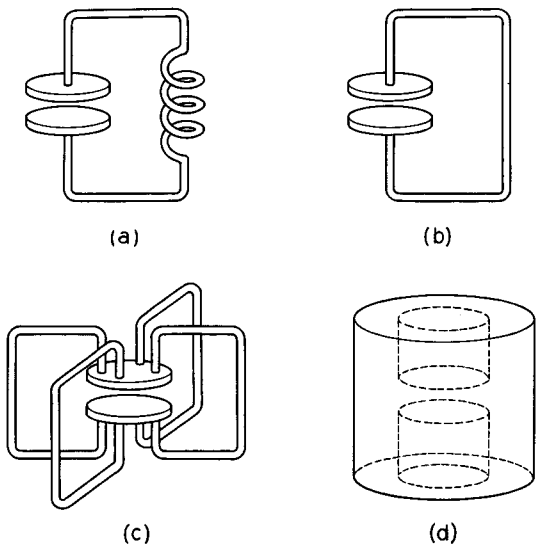

FIG. 8-1 Evolution of a cavity resonator from its low-frequency prototype. (a) Low-frequency prototype. (b) Inductance decreased to that of a single turn wire. (c) Single wires in parallel, reducing the inductance further. (d) Cavity resonator resulting from a continuation of the process of Figure 8-1(c).

relating to beam spreading and confining the beam with external fields, as discussed in Section 3.4. This determines a minimum area for the electrodes. As the frequency is further increased, therefore, one must resort to reducing the inductance. However, we soon reach the point where the inductance is a single short wire, as shown in Figure 8-1(b). Still higher resonant frequencies can be obtained by paralleling the single wire with additional single-wire inductances, as indicated in Figure 8-1(c). As this procedure is carried to the limit, one obtains the re-entrant cavity structure shown in Figure 8-1(d). A cross-sectional view of such a cavity is shown in Figure 8-2. Such resonant cavities are used in klystrons and microwave triodes and tetrodes. Not only has the inductance been decreased in the resonant cavity, but also the resistance losses are lessened, and the self-shielding configuration prevents radiation losses. The fact that all of the electromagnetic fields are confined to the interior of the cavity will become more obvious after a discussion of "skin effect."

To calculate the resonant frequency of a cavity such as that shown in Figure 8-2 is often a difficult process.[1] However, approximate calculations

[1]References 8.1, 8.4.

can often be made to obtain useful information. For instance, we note that in the cavity shown in Figure 8-2, the capacitive gap is short compared with its diameter. This cavity may be thought of as two shorted coaxial lines joined by a capacitance. It can be shown that the input impedance to each shorted coaxial line is given by the expression[2]

$$Z_{\text{in}} = \frac{j}{2\pi}\sqrt{\frac{\mu_o}{\varepsilon_o}} \ln\frac{a}{b} \tan\frac{\omega l}{c} \qquad (8\text{-}1)$$

where $c = 1/\sqrt{\mu_o\varepsilon_o}$ is the velocity of light. The capacitance of the gap is given by the expression

$$C_g = \frac{\varepsilon_o \pi b^2}{h} \qquad (8\text{-}2)$$

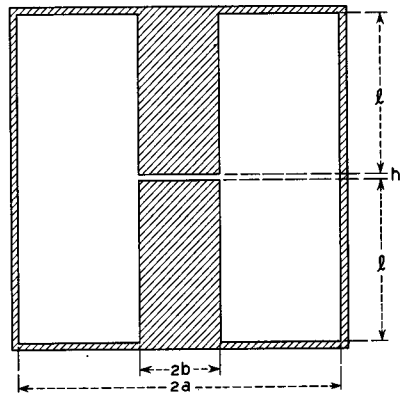

FIG. 8-2 Re-entrant cavity resonator which can be analyzed by simple transmission line theory. The cavity is airfilled.

where fringing effects are neglected. At resonance, the inductive reactance of the two shorted coaxial lines in series is equal in magnitude to the capacitive reactance of the gap, but of opposite sign. Hence,

$$\frac{j}{\pi}\sqrt{\frac{\mu_o}{\varepsilon_o}}\left(\ln\frac{a}{b}\right)\tan\frac{\omega l}{c} - j\frac{h}{\omega\varepsilon_o\pi b^2} = 0 \qquad (8\text{-}3)$$

The solution to this equation gives the resonant frequency. Rearranging the equation, we obtain

$$\frac{\omega l}{c}\tan\frac{\omega l}{c} = \frac{hl}{b^2 \ln\frac{a}{b}} \qquad (8\text{-}4)$$

For the particular set of dimensions given by $a = l$, $h = 0.0318l$, and $a = 4b$, Equation (8-4) is satisfied by $\omega l/c = 0.571$, and we can scale the dimensions to suit any frequency. At 3000 Mc, l is equal to 0.91 cm. This sort of scaling operation is a general property of microwave components. That is, if we multiply all dimensions by a factor K, all frequencies of interest are divided by K.

In the above example, the solution $\omega l/c = 0.571$ is equivalent to saying that l is 0.0908 wavelength long. It can be shown that averaged over a cycle, a shorted coaxial line of this length contains 8.84 times as much

[2]Reference 8.2.

magnetic stored energy as it contains electric energy. The balance of the electric stored energy appears in the gap, since at resonance the electric and magnetic stored energies are equal in magnitude (but 90 degrees out of time phase). The region outside of the gap is called the inductive region of the cavity, and to a good approximation it can be considered to have only magnetic fields. The cavity can therefore be represented by the equivalent circuit of Figure 8-1(a), where the capacitance C is the gap capacitance, and the inductance is chosen to give the correct resonant frequency.

Since Equation (8-4) contains the tangent function, it has an infinite number of solutions with larger values of frequency. Physically, this corresponds approximately to additional half wavelengths on the coaxial line at higher frequencies. This behavior is typical of all microwave cavities; that is, there are an infinite number of resonant frequencies or modes of oscillation. However, resonant cavities are nearly always operated in the lowest frequency, or dominant, mode because the resistive losses are usually lower in that mode. Resistive losses in the cavity can be represented in the equivalent circuit of Figure 8-1(a) by a parallel resistance of such a value as to give the correct power loss per cycle for a given amount of stored energy.

Next let us consider the problem of transmitting microwave energy from one point to another with as little resistive and radiation losses as possible. Radiation losses can be kept to a minimum by using a suitable form of transmission line, such as a coaxial line, stripline, or a waveguide. Of these types of transmission line, the waveguide is capable of giving minimum attenuation per unit length at a given signal frequency, and it is the most commonly used form of transmission line at microwave frequencies. A study of wave propagation in a waveguide provides a suitable introduction to a discussion of wave propagation along other forms of transmission line such as are used in microwave tubes.

Our principal mathematical tool for studying the transport of electromagnetic energy from one point to another is a set of equations, known as *Maxwell's Equations*. These equations can be used to describe electromagnetic wave propagation in free space, and in principle they can be used to describe electromagnetic wave propagation along an arbitrarily shaped transmission line. We shall first consider the plane electromagnetic wave in free space and then show that electromagnetic wave propagation in a waveguide can be considered as a superposition of two plane electromagnetic waves.

Suppose the direction of propagation of a plane electromagnetic wave is taken to be the z direction. With proper choice of the rectangular coordinate system, the wave consists of an electric field component E_x and a magnetic field component H_y, both of which vary sinusoidally in the z

direction with wavelength $\lambda_o = c/f$, where c is the velocity of propagation, and f is the frequency of the signal. For a plane wave in free space H_y is related to E_x by $H_y = (\sqrt{\varepsilon_o/\mu_o})E_x$. The power density flowing in the z direction is equal to $|E_x|\,|H_y|$ watts per square meter of wave front.

Figure 8-3 shows the field lines associated with two plane waves of equal amplitude. One wave is propagating upwards and to the right with velocity

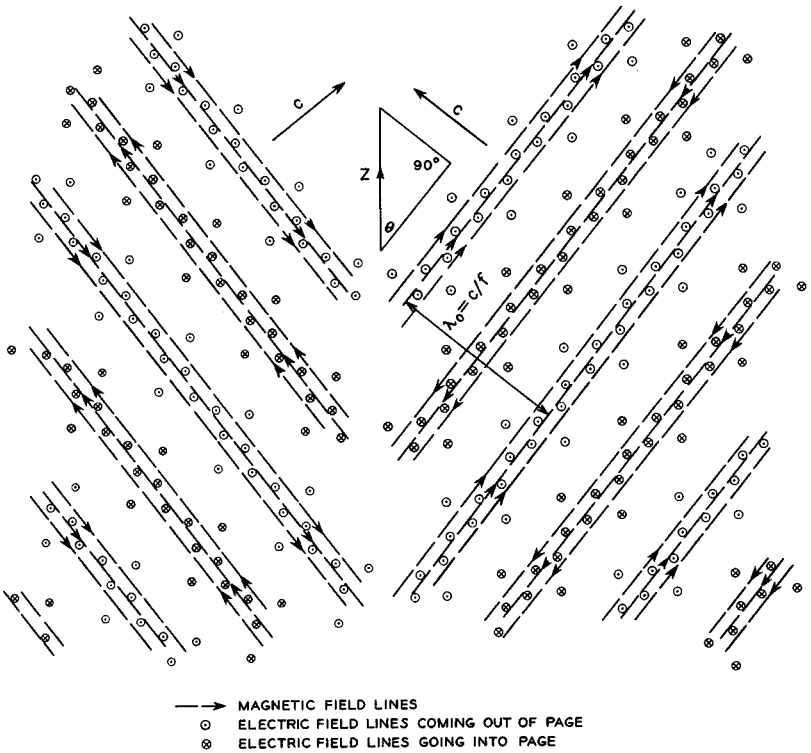

FIG. 8-3 Two plane waves. One is advancing upwards and to the right with velocity c, and one is advancing upwards and to the left with velocity c.

c, and one is propagating upwards and to the left with velocity c. Each wave front makes an angle θ with the vertical, or z, direction. Maxwell's Equations are linear, so that the field pattern resulting from a superposition of the two waves is obtained by a vector addition of the individual field components. Figure 8-4 shows the field pattern which results from this vector addition.

The field pattern of Figure 8-4 moves only in the z direction. Examination of the vector diagram shown in the upper right-hand part of the

figure shows that, in the time taken for an individual plane wave to travel the distance EF, the field pattern of Figure 8-4 travels in the z direction a distance EG. Thus the *phase velocity* of the field pattern in Figure 8-4 is given by $v_p = c/\sin\theta$. On the other hand, the electromagnetic energy associated with the individual plane waves propagates in the direction of

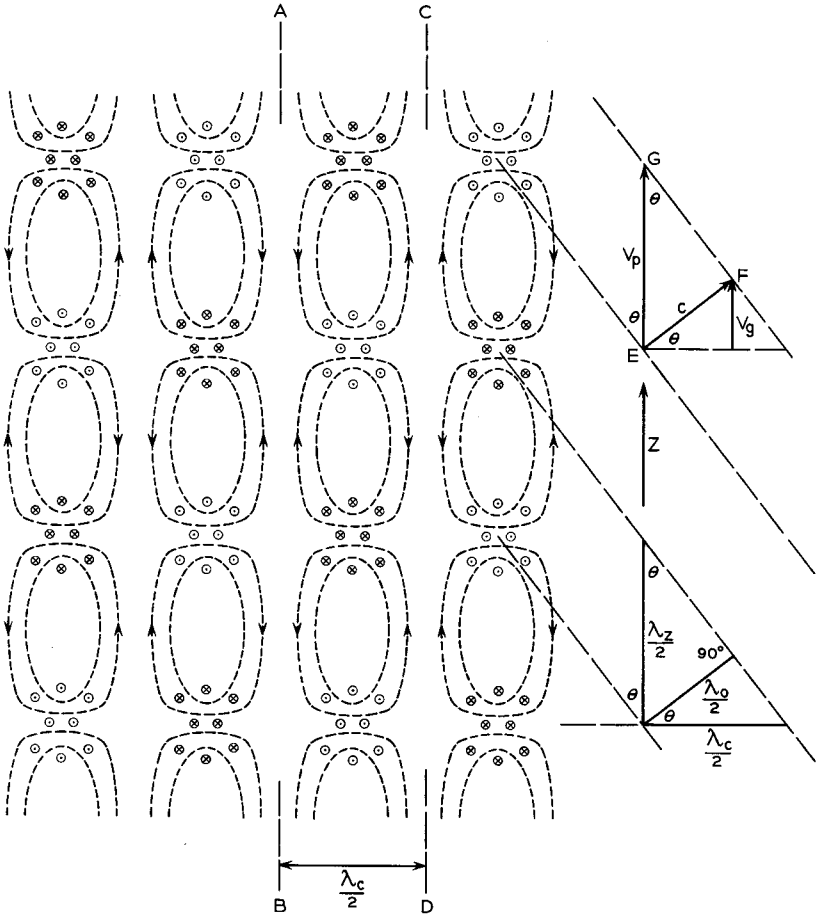

FIG. 8-4 A superposition of the two plane waves shown in Figure 8-3. With increasing time the whole pattern moves in the z direction with *phase velocity* $v_p = c/\sin\theta$. The wavelength in the z direction is given by $\lambda_z = \lambda_o/\sin\theta$. The energy associated with the two separate waves propagates in the direction of travel of the wave fronts of the separate waves. This direction makes an angle of $90° - \theta$ with the z direction. Hence, the energy associated with the above pattern propagates in the z direction with a *group velocity* given by $v_g = c \cos (90° - \theta = c \sin\theta$.

travel of the wave fronts and hence at an angle of $90 - \theta$ degrees with respect to the z direction. Since one wave transports electromagnetic energy to the right and upwards, and the other wave transports electromagnetic energy to the left and upwards, the *net* transport of energy is in the z direction only. The velocity with which the energy is transported in the z direction is given by the *group velocity* $v_g = c \cos(90° - \theta) = c \sin\theta$.

The wavelength λ_z of the field pattern in Figure 8-4 is easily seen to be related to the free-space wavelength λ_o by $\lambda_z = \lambda_o/\sin\theta$.

From Figure 8-4 it is evident that the electric field intensity is zero along the planes AB and CD at all times, and the magnetic field lines never cross the planes. Hence, if thin conducting sheets were inserted along these planes, the field pattern would not be disturbed. In this case the two plane waves between the conducting sheets reflect from one side to another, at the same time progressing in the z direction. The plane waves outside the conducting sheets are likewise reflected from the conducting sheets, and the net result is that the field pattern of Figure 8-4 is undisturbed.

Next, let us remove the field pattern for a moment and suppose we have two conducting plates of very large area and spaced by the distance from plane AB to plane CD in Figure 8-4. Suppose that two plane waves are launched *between* the plates with the E field parallel to the plates and with the wave fronts making an angle θ with the surface of the plates. The angle between the two wave fronts is then 2θ, as in Figure 8-3. The two waves are reflected from plate to plate, and the resulting field pattern is identical to that shown between the planes AB and CD in Figure 8-4.

Finally, suppose that the two "side plates" of the previous paragraph are joined by "top" and "bottom" plates to form a rectangular waveguide, as shown in Figure 8-5. The electric field lines now terminate on surface charges on the top and bottom plates, but the shape of the field pattern is otherwise unchanged. The waves propagate along the waveguide with phase velocity $v_p = c/\sin\theta$, and the electromagnetic energy propagates with the group velocity given by $v_g = c \sin\theta$. The axial wavelength of the field pattern in the waveguide is given by $\lambda_z = \lambda_o/\sin\theta$.

What we have done here is to find a field pattern that satisfies the boundary conditions imposed by the rectangular waveguide. These boundary conditions require that the tangential component of electric field intensity at the surface of the conducting walls be zero, and the normal component of magnetic field intensity at the surface of the waveguide be zero. From Figure 8-4 it is evident that the distance between planes AB and CD is determined by the angle θ and the wavelength λ_o of the plane waves. Conversely, if we have a waveguide of a given width a and a given wavelength λ_o, the angle θ is determined. If we set the width a of the waveguide equal to $\lambda_c/2$, it is evident from Figure 8-4 that $\cos\theta = \lambda_o/\lambda_c$, and hence

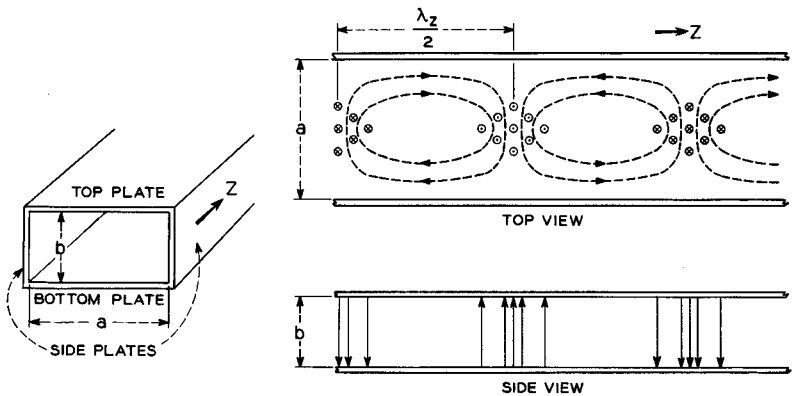

FIG. 8-5 Field patterns in a rectangular waveguide. The broken lines indicate the shapes of the magnetic field lines, and the solid lines indicate the shapes of the electric field lines.

$\sin\theta = \sqrt{1 - \cos^2\theta} = \sqrt{1 - \lambda_o^2/\lambda_c^2}$. Thus we have the relations

$$v_p = \frac{c}{\sqrt{1 - \lambda_o^2/\lambda_c^2}} \tag{8-5}$$

$$v_g = c\sqrt{1 - \lambda_o^2/\lambda_c^2} \tag{8-6}$$

and

$$\lambda_z = \frac{\lambda_o}{\sqrt{1 - \lambda_o^2/\lambda_c^2}} \tag{8-7}$$

So far we have described only the most frequently used dominant mode of propagation of waves in a rectangular waveguide. From Figure 8-4 it is evident that waves in this mode can propagate only if λ_o is less than λ_c. We also note that Equations (8-5) and (8-6) indicate that v_p and v_g become imaginary quantities when $\lambda_o > \lambda_c$. The wavelength λ_c is called the cutoff wavelength and is a characteristic of the waveguide and the mode of propagation. Signals of wavelength shorter than λ_c can propagate, but signals of longer wavelength cannot propagate. (We assume here that the dimension b of the waveguide is smaller than a.)

Finally, let us return once more to Figure 8-4. Suppose the plane CD were translated to the right a distance $\lambda_c/2$. The field pattern between the planes would then consist of two side-by-side patterns similar to the one described above for the dominant mode of the rectangular waveguide. Clearly this field pattern also satisfies the boundary conditions of an *enlarged* waveguide, that is, one twice as wide as we have previously considered. Or, conversely, for a given waveguide width, such a field pattern

can be established in the waveguide provided the free space wavelength of the signal is sufficiently short. In a similar way, we see that an infinite number of field patterns or modes of propagation can be established in a rectangular waveguide. As the field pattern becomes more complex, the cutoff wavelength becomes shorter, and the signal frequency must be higher. Furthermore, since waves can be reflected from the top and bottom of the rectangular waveguide, there is a second infinite set of modes of propagation in which the electric field lines are parallel to the a dimension of the waveguide. Also, for a given signal frequency, a mode with the **E** field parallel to the a dimension can be superimposed on a mode with the **E** field parallel to the b dimension. The resulting field patterns, therefore, can be very complex. Later in the chapter we shall find that there are still other modes of propagation in which the **E** field has a z component and the **H** field is entirely transverse to the z direction.

The final section of the chapter considers the propagation of electromagnetic waves along transmission lines which are characterized by phase velocities that are less than the velocity of light. Such transmission lines form integral parts of a number of microwave tubes, such as traveling-wave tubes, backward-wave oscillators, and magnetrons.

8.1 Maxwell's Equations and the Wave Equation

Some of the laws governing the behavior of static electric and magnetic fields were discussed in Chapter 1. The equations from that chapter which are pertinent to our present discussion are listed below.

Equation (1.1-4): $$\oint_{\text{closed path}} \mathbf{E}\cdot d\mathbf{l} = 0 \tag{8.1-1}$$

Equation (1.4-3): $$\nabla\cdot\mathbf{D} = \rho \tag{8.1-2}$$

Equation (1.5-2): $$\nabla\cdot\mathbf{B} = 0 \tag{8.1-3}$$

Equation (1.5-5): $$\nabla\times\mathbf{H} = \mathbf{J} \tag{8.1-4}$$

We shall consider these equations one by one to see what form they take when time-varying fields are present.

First, it may be stated that Equations (8.1-2) and (8.1-3) are true as they stand for time-varying fields and charges as well as for static fields and charges.

Let us next consider Equation (8.1-1) as it applies to a closed loop of resistance wire. The experiments of Faraday have shown that, if the loop is linked by changing magnetic fields, there will be current flow around the loop and hence a voltage drop around the loop. That is to say, the right-

hand side of Equation (8.1-1) is not equal to zero in such a time-varying field. Faraday's law may be stated mathematically as

$$\oint_{\text{closed path}} \mathfrak{E} \cdot d\mathbf{l} = -\frac{\partial}{\partial t} \int_{\text{surface}} \mathfrak{B} \cdot \mathbf{n} dS \tag{8.1-5}$$

where the surface of integration is taken as any surface bounded by the closed path. Script letters are used for the time-varying field vectors to distinguish them from the dc vectors used previously. Physically the law states that the total voltage induced in a closed loop is given by the time rate of change of magnetic flux linking the loop. We can convert this equation to a more useful form by applying it to a small loop of area ΔA, the loop being small enough that $\mathfrak{B}$ can be taken as uniform in magnitude and direction. Let the component of $\mathfrak{B}$ normal to the plane of the loop be denoted by $\mathfrak{B}_n$. Dividing both sides of the equation by ΔA and taking the limit as $\Delta A \to 0$, we have

$$\lim_{\Delta A \to 0} \frac{1}{\Delta A} \oint_{\text{closed path}} \mathfrak{E} \cdot d\mathbf{l} = -\frac{\partial \mathfrak{B}_n}{\partial t} \tag{8.1-6}$$

But the left-hand side is equal to the component of $\nabla \times \mathfrak{E}$ normal to the plane of the loop, so that

$$\nabla \times \mathfrak{E} = -\frac{\partial \mathfrak{B}}{\partial t} \tag{8.1-7}$$

Expressions for the curl in rectangular and cylindrical coordinate systems are given in Appendix XII.

Maxwell's great contribution to these fundamental laws was a recognition of the fact that ac magnetic fields are set up not only by real currents consisting of charges in motion, but also by so-called displacement currents. The displacement current density is given by the time rate of change of the electric flux density vector $(\partial/\partial t)\ \mathfrak{D}$, so that Equation (8.1-4) becomes

$$\nabla \times \mathfrak{H} = \mathfrak{J} + \frac{\partial \mathfrak{D}}{\partial t} \tag{8.1-8}$$

If we take the divergence of both sides of Equation (8.1-8), we obtain

$$\nabla \cdot \left(\mathfrak{J} + \frac{\partial \mathfrak{D}}{\partial t} \right) = 0$$

since the divergence of a curl is identically zero. Using Gauss's Law, Equation (8.1-2), this may be written as

$$\nabla \cdot \mathfrak{J} + \frac{\partial \rho}{\partial t} = 0$$

the equation of continuity, Equation (1.3-2). Thus, the introduction of the displacement current density in Equation (8.1-8) is necessary to satisfy the equation of continuity.

We may thus summarize our results for ac and dc fields in the four equations known as Maxwell's equations:

$$\nabla \times \mathcal{E} = -\frac{\partial \mathcal{B}}{\partial t} \tag{8.1-9}$$

$$\nabla \times \mathcal{H} = \mathcal{J} + \frac{\partial \mathcal{D}}{\partial t} \tag{8.1-10}$$

$$\nabla \cdot \mathcal{D} = \rho \tag{8.1-11}$$

$$\nabla \cdot \mathcal{B} = 0 \tag{8.1-12}$$

Equations (8.1-9) and (8.1-10) when taken together, with conduction current density $\mathcal{J}$ set to zero, form a very interesting pair. Equation (8.1-9) states that a changing magnetic field gives rise to an electric field, and Equation (8.1-10) in turn states that a changing electric field gives rise to a magnetic field. Thus it is clear how wave propagation and standing-wave phenomena are obtained: each type of electromagnetic field vector acts as a source for the other. A change in one produces the other, and vice versa. Thus, energy oscillates continuously from the electric fields to the magnetic fields and back.

In all our discussions of microwave tubes we shall describe physical behavior for a simple sinusoidal variation at a fixed frequency. In all cases we shall be dealing with linear phenomena, and hence we can represent any arbitrary input or response by a superposition of sinusoidal inputs and responses. We can therefore use the *phasor* notation to describe the currents and field vectors:

$$\mathcal{E} = \text{Re}\, \mathbf{E}\epsilon^{j\omega t}, \qquad \mathcal{J} = \text{Re}\, \mathbf{J}\epsilon^{j\omega t}, \text{ etc.}$$

Then

$$\frac{\partial \mathcal{E}}{\partial t} = \text{Re}\, j\omega \mathbf{E}\epsilon^{j\omega t}, \text{ etc.} \tag{8.1-13}$$

Thus, if all quantities vary sinusoidally at a single frequency, we have the following form of Maxwell's Equations:

$$\nabla \times \mathbf{E} = -j\omega \mathbf{B} \tag{8.1-14}$$

$$\nabla \times \mathbf{H} = \mathbf{J} + j\omega \mathbf{D} \tag{8.1-15}$$

$$\nabla \cdot \mathbf{D} = \rho \tag{8.1-16}$$

$$\nabla \cdot \mathbf{B} = 0 \tag{8.1-17}$$

In rectangular coordinates Equations (8.1-14) and (8.1-15) can be written as

$$\frac{\partial E_z}{\partial y} - \frac{\partial E_y}{\partial z} = -j\omega\mu\mu_o H_x$$

$$\frac{\partial E_x}{\partial z} - \frac{\partial E_z}{\partial x} = -j\omega\mu\mu_o H_y$$

$$\frac{\partial E_y}{\partial x} - \frac{\partial E_x}{\partial y} = -j\omega\mu\mu_o H_z \tag{8.1-18}$$

and

$$\frac{\partial H_z}{\partial y} - \frac{\partial H_y}{\partial z} = J_x + j\omega\varepsilon\varepsilon_o E_x$$

$$\frac{\partial H_x}{\partial z} - \frac{\partial H_z}{\partial x} = J_y + j\omega\varepsilon\varepsilon_o E_y$$

$$\frac{\partial H_y}{\partial x} - \frac{\partial H_x}{\partial y} = J_z + j\omega\varepsilon\varepsilon_o E_z \tag{8.1-19}$$

where we have substituted $\mathbf{B} = \mu\mu_o\mathbf{H}$ in Equation (8.1-14) and $\mathbf{D} = \varepsilon\varepsilon_o\mathbf{E}$ in Equation (8.1-15).

In addition to Equations (8.1-14) through (8.1-17), it should be noted that two other equations from Chapter 1 are valid for time-varying fields as well as for dc fields. These are the equations for the force on an electron, Section 1.2, and the equation of continuity, Equation (1.3-2), which in phasor notation becomes

$$\nabla\cdot\mathbf{J} = -j\omega\rho \tag{8.1-20}$$

Let us now use Equations (8.1-14) and (8.1-15) to derive the wave equation for an electromagnetic wave in a region in which there are no free charges and no conduction currents. In this case the equations reduce to

$$\nabla\times\mathbf{E} = -j\omega\mu\mu_o\mathbf{H} \tag{8.1-21}$$

$$\nabla\times\mathbf{H} = j\omega\varepsilon\varepsilon_o\mathbf{E} \tag{8.1-22}$$

Taking the curl of both sides of the first equation and combining the result with the second equation, we obtain

$$\nabla\times(\nabla\times\mathbf{E}) = -j\omega\mu\mu_o\nabla\times\mathbf{H} = \omega^2\mu\mu_o\varepsilon\varepsilon_o\mathbf{E} \tag{8.1-23}$$

Now from Equation 13 of Appendix XII,

$$\nabla\times(\nabla\times\mathbf{E}) = \nabla(\nabla\cdot\mathbf{E}) - \nabla^2\mathbf{E} \tag{8.1-24}$$

The first term on the right here is zero since, from Equation (8.1-16),

$$\nabla\cdot\mathbf{E} = \frac{\rho}{\varepsilon\varepsilon_o} \tag{8.1-25}$$

and we have assumed $\rho = 0$ in the region of space under consideration, Equation (8.1-23) then can be written as

$$\nabla^2\mathbf{E} + k^2\mathbf{E} = 0 \tag{8.1-26}$$

where $k^2 = \omega^2\mu\mu_o\varepsilon\varepsilon_o$. This equation is known as the wave equation for an electric field. Equations (8.1-21) and (8.1-22) also can be used in a similar manner to derive the wave equation for a magnetic field, namely

$$\nabla^2\mathbf{H} + k^2\mathbf{H} = 0 \tag{8.1-27}$$

Equations (8.1-26) and (8.1-27) describe the propagation of an electromagnetic wave in a region of free space in which there are no free charges or conduction currents.

Perhaps the simplest application of Equations (8.1-26) and (8.1-27) is in the description of a plane electromagnetic wave, such as one might obtain at a very large distance from a radiating antenna. Let us assume that the electric field intensity of the wave is directed only in the x direction and is given by E_x. For a wave propagating in the z direction, Equation (8.1-26) then reduces to

$$\frac{d^2E_x}{dz^2} + k^2E_x = 0 \tag{8.1-28}$$

This has the solution

$$E_x = E_{xo}\epsilon^{\pm jkz} \tag{8.1-29}$$

Now $k^2 = \omega^2\mu\mu_o\varepsilon\varepsilon_o$, and in free space $\mu = \varepsilon = 1$. We shall set $k = \omega/c$ for a wave in free space, where $c = 1/\sqrt{\mu_o\varepsilon_o}$. If time dependence is included, and if we assume the propagating medium is free space, the expression for the electric field intensity becomes

$$\mathcal{E}_x = \text{Re } E_{xo}\epsilon^{j(\omega t \pm kz)} = \text{Re } E_{xo}\epsilon^{j\omega[t \pm (z/c)]} = E_{xo}\cos\omega\left(t \pm \frac{z}{c}\right) \tag{8.1-30}$$

Here the plus sign in the term $\cos\omega[t \pm (z/c)]$ applies to a wave propagating in the negative z direction, and the minus sign applies to a wave propagating in the positive z direction. We see that the quantity $c = 1/\sqrt{\mu_o\varepsilon_o}$ is the velocity of propagation of the plane wave, equal to 3×10^8 meters/sec.

By setting $E_y = E_z = 0$ in Equation (8.1-18), we find that $H_x = H_z = 0$, and

$$H_y = \frac{j}{\omega\mu_o}\frac{\partial E_x}{\partial z} = \frac{k}{\omega\mu_o}E_x = \sqrt{\frac{\varepsilon_o}{\mu_o}}E_x \tag{8.1-31}$$

where we have assumed a wave propagating in the positive z direction and have used a minus sign in the exponent on the right-hand side of Equation

(8.1-29). We have also assumed that $\mu = \varepsilon = 1$. Equation (8.1-31) indicates that *for a plane wave propagating in free space, the ratio of the electric field intensity to the magnetic field intensity is given by* $\sqrt{\mu_o/\varepsilon_o}$. This ratio has the dimensions of an impedance and is numerically equal to 377 ohms.

8.2 Energy Stored in Electric and Magnetic Fields; Power Flow in an Electromagnetic Wave

Here we shall first derive expressions for the energy stored per unit volume in electric and magnetic fields. The expressions apply to both static and time-varying fields.[3]

(*a*) *Electric Fields*

Consider a capacitor that is charged to a voltage of v volts. If an incremental amount of charge dq is added to the charge already on the capacitor, the work done in adding the incremental charge is vdq. This work is converted to energy stored in the electric field of the capacitor. Now from Equation (1.4-7) we have $q = Cv$, and hence $dq = Cdv$. Thus the work done in adding the charge dq to the capacitor is $Cvdv$. If the capacitor is charged from zero volts to v volts, the energy stored in the electric field of the capacitor is given by

$$\text{energy stored} = \int_o^v Cvdv = \tfrac{1}{2}Cv^2 \qquad (8.2\text{-}1)$$

If the capacitor is a parallel-plate device in which the plates are of area A and spacing d, and if edge effects are neglected, $C = \varepsilon\varepsilon_o A/d$, and the energy stored per unit volume between the plates is $\frac{1}{2}Cv^2/Ad = \frac{1}{2}\varepsilon\varepsilon_o(v/d)^2$. Setting $v/d = \mathcal{E}$, where $\mathcal{E}$ is the electric field intensity between the plates, we obtain

$$\text{energy stored per unit volume} = \tfrac{1}{2}\varepsilon\varepsilon_o\mathcal{E}^2 \qquad (8.2\text{-}2)$$

We see that the expression for the energy stored per unit volume depends only on the magnitude of the electric field intensity and is independent of the geometry of the electrodes that generate the field.

(*b*) *Magnetic Fields*

Equation (8.1-5) indicates that the voltage induced in a loop of resistance wire by a changing magnetic field is equal to the time rate of change of the magnetic flux linking the loop. Consider a toroidal coil, such as that shown in Figure 1.5-3. If the coil has N turns and all are linked by the flux ϕ, the

[3]References 8a, 8c, 8d.

voltage induced in the coil by a changing ϕ is given by

$$v = N\frac{d\phi}{dt} \tag{8.2-3}$$

Now the inductance L of the coil is equal to the number of flux linkages per ampere of current passing through the coil. Hence $N\phi = Li$, and

$$Nd\phi = Ldi \tag{8.2-4}$$

Equation (8.2-3) then can be written as

$$v = L\frac{di}{dt} \tag{8.2-5}$$

This equation states that when the current through the coil is changing, there is a voltage v developed across the coil proportional to the rate of change of the current. (The resistive losses in the coil are neglected here.)

The rate at which work is being done to change the current in the coil is vi. Thus the work done in an increment of time dt during which the current changes by di is $vidt = Lidi$. This work is converted to energy stored in the magnetic field of the coil. The total energy stored in the magnetic field when the current in the coil is increased from zero to i is then

$$\text{energy stored} = \int_0^i Lidi = \tfrac{1}{2}Li^2 \tag{8.2-6}$$

In the case of the toroidal coil shown in Figure 1.5-3, $L = \pi r^2\mu\mu_o nN$, where r is the radius of the individual turns of wire, μ is the relative permeability of the medium filling the coil, n is the number of turns per unit length around the coil, and N is the total number of turns in the coil. If R is the mean radius of the toroid, $n = N/2\pi R$. The volume within which the magnetic energy is stored is approximately given by $(\pi r^2)(2\pi R)$. Hence the energy stored per unit volume within the coil is given by $\frac{1}{2}Li^2/(\pi r^2)(2\pi R)$, which reduces to

$$\text{energy stored per unit volume} = \tfrac{1}{2}\mu\mu_o(ni)^2 = \tfrac{1}{2}\mu\mu_o\mathcal{H}^2 \tag{8.2-7}$$

where we have substituted $\mathcal{H} = ni$ from Equation (1.5-11). Again we see that the energy stored per unit volume depends only on the magnitude of the magnetic field intensity and is independent of the field configuration.

(c) *Power Flow in an Electromagnetic Wave*

Here we shall examine the power flow associated with a plane wave propagating in free space. We shall assume that the wave propagation is in the z direction and consists of an electric field component $\mathcal{E}_x$ and a magnetic field component $\mathcal{H}_y$. Consider a pillbox element of volume with faces of area A

lying parallel to the x-y plane and having thickness dz in the z direction. The energy stored in this volume will vary with time as the wave propagates past the volume element. From Equations (8.2-2) and (8.2-7), the instantaneous stored energy in the volume element is given by

$$\mathcal{W} = \tfrac{1}{2}(\varepsilon_o \mathcal{E}_x^2 + \mu_o \mathcal{H}_y^2) A\,dz \tag{8.2-8}$$

The rate of change of energy stored in the volume element is

$$\begin{aligned}\frac{\partial \mathcal{W}}{\partial t} &= A\,dz\left(\varepsilon_o \mathcal{E}_x \frac{\partial \mathcal{E}_x}{\partial t} + \mu_o \mathcal{H}_y \frac{\partial \mathcal{H}_y}{\partial t}\right) \\ &= -A\,dz\left(\mathcal{E}_x \frac{\partial \mathcal{H}_y}{\partial z} + \mathcal{H}_y \frac{\partial \mathcal{E}_x}{\partial z}\right) \\ &= -A\,dz \frac{\partial}{\partial z}(\mathcal{E}_x \mathcal{H}_y)\end{aligned} \tag{8.2-9}$$

where we have substituted $\varepsilon_o(\partial \mathcal{E}_x/\partial t) = -\partial \mathcal{H}_y/\partial z$ from Equation (8.1-10) and $\mu_o(\partial \mathcal{H}_y/\partial t) = -\partial \mathcal{E}_x/\partial z$ from Equation (8.1-9).

Thus the time rate of change of the energy stored in the volume element is equal to the change in the quantity $A\mathcal{E}_x\mathcal{H}_y$ in the distance dz. Since energy flows only in the z direction, we see that $\mathcal{E}_x\mathcal{H}_y$ is of the nature of a *power density*, or rate of flow of energy per unit area. It is customary to represent the power density by a vector $\mathbf{S}$, which is directed in the direction of propagation. In the present case,

$$|\,\mathbf{S}\,| = S_z = \mathcal{E}_x \mathcal{H}_y \tag{8.2-10}$$

More generally, whenever there is propagation of electromagnetic energy, the power density can be represented by a vector $\mathbf{S}$ such that

$$\mathbf{S} = \boldsymbol{\mathcal{E}} \times \boldsymbol{\mathcal{H}} \tag{8.2-11}$$

The vector $\mathbf{S}$ is called the *Poynting vector* after the man who discovered it. The power density is measured in watts per square meter.

Equation (8.2-10) can be written in another useful form as follows:

$$S_z = \frac{1}{2}(\mathcal{E}_x \mathcal{H}_y + \mathcal{E}_x \mathcal{H}_y) = \frac{1}{2}\left[\sqrt{\frac{\varepsilon_o}{\mu_o}}\mathcal{E}_x^2 + \sqrt{\frac{\mu_o}{\varepsilon_o}}\mathcal{H}_y^2\right] = c\left[\frac{1}{2}\varepsilon_o \mathcal{E}_x^2 + \frac{1}{2}\mu_o \mathcal{H}_y^2\right] \tag{8.2-12}$$

where we have substituted $\mathcal{E}_x = \sqrt{\mu_o/\varepsilon_o}\ \mathcal{H}_y$ from Equation (8.1-31) and $c = 1/\sqrt{\mu_o \varepsilon_o}$. This states that the energy stored in the electric and magnetic fields of the plane wave propagates in the z direction with velocity c, as we might expect.

8.3 Boundary Conditions

Maxwell's Equations constitute a set of differential equations which can be solved in a given region subject to imposed boundary conditions. In

many cases, the region over which a solution is sought can be divided up into several subregions, and appropriate matching of fields is made at the boundaries between these regions. Let us therefore consider the relationships between the fields adjacent to a boundary but on either side of it.

(a) *Electric Fields*

Figure 8.3-1(a) shows the boundary between two regions of different relative dielectric constants ε_A and ε_B. A single electric field line passing through the boundary between the two regions is shown. In region A the electric field has magnitude E_A, and in region B it has magnitude E_B. A small rectangle is drawn about the point where the field line crosses the boundary. The rectangle is Δz units long in the direction parallel to the boundary and Δx units wide in the direction normal to the boundary. Half of the rectangle is in each region. We shall assume that $\mathbf{E}_A$ can be resolved into two components, one parallel to the boundary $E_{\|A}$, and one normal to the boundary $E_{\perp A}$. Similarly, $\mathbf{E}_B$ can be resolved into components $E_{\|B}$ and $E_{\perp B}$.

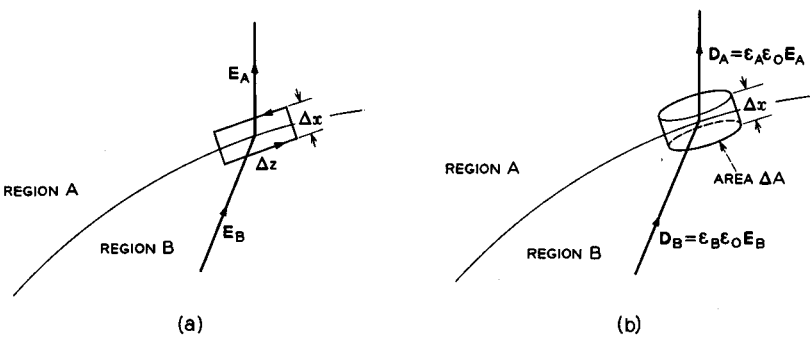

FIG. 8.3-1 Electric field vectors at a point on the boundary between two regions. Region A has permittivity $\varepsilon_A\varepsilon_o$ and region B has permittivity $\varepsilon_B\varepsilon_o$.

Let us evaluate Equation (8.1-5) for the region defined by the rectangle $\Delta x \Delta z$ in Figure 8.3-1(a). Substituting $\mathcal{E} = \text{Re}\ \mathbf{E}\ \epsilon^{j\omega t}$ and $\mathcal{B} = \text{Re}\ \mathbf{B}\ \epsilon^{j\omega t}$ in the equation, we obtain

$$\oint_{\text{closed loop}} \mathbf{E}\cdot d\mathbf{l} = -j\omega \int_{\text{surface}} \mathbf{B}\cdot\mathbf{n}dS \qquad (8.3\text{-}1)$$

If both Δx and Δz are assumed to be very small, $\mathbf{E}$ in region A or region B will be constant in magnitude and direction over the part of the rectangle included in the region. Let the average value of the component of $\mathbf{B}$

normal to the plane of the rectangle be B_n. Equation (8.3-1) can then be written

$$\oint_{\text{rectangle}} \mathbf{E}\cdot d\mathbf{l} = E_{\|B}\Delta z + E_{\perp B}\frac{\Delta x}{2} + E_{\perp A}\frac{\Delta x}{2} - E_{\|A}\Delta z - E_{\perp A}\frac{\Delta x}{2} - E_{\perp B}\frac{\Delta x}{2}$$
$$= -j\omega B_n \Delta x \Delta z \tag{8.3-2}$$

Next let $\Delta x \to 0$ in such a way that the rectangle is still centered about the boundary. The right-hand side of Equation (8.3-2) then approaches zero, and the equation reduces to

$$E_{\|B}\Delta z - E_{\|A}\Delta z = 0 \tag{8.3-3}$$

from which

$$E_{\|A} = E_{\|B} \tag{8.3-4}$$

Thus the components of **E** parallel to the boundary are equal on both sides of the boundary, despite the fact that the two regions have different dielectric constants.

Next let us consider the field perpendicular to the boundary. We shall work with the **D** vector in this case and show that the normal component of **D** is continuous at the boundary. Figure 8.3-1(b) shows an electric field line which passes through the boundary between regions A and B. In region A, $\mathbf{D}_A = \varepsilon_A\varepsilon_o\mathbf{E}_A$, and in region B, $\mathbf{D}_B = \varepsilon_B\varepsilon_o\mathbf{E}_B$. A small pillbox-shaped volume surrounds the point where the field line passes through the boundary. The pillbox has area ΔA on the faces parallel to the boundary and thickness Δx. We assume that $\mathbf{D}_A$ can be resolved into a component $D_{\perp A}$ perpendicular to the boundary and $D_{\|A}$ parallel to the boundary. Similarly, $\mathbf{D}_B$ can be resolved into $D_{\perp B}$ and $D_{\|B}$.

Equation (8.1-16) can be written in the form

$$\int_{\text{volume}} \nabla\cdot\mathbf{D}dv = \int_{\text{volume}} \rho dv \tag{8.3-5}$$

Using Gauss's theorem (Appendix XII) this may be written as

$$\int_{\text{closed surface}} \mathbf{D}\cdot\mathbf{n}dS = \int_{\text{volume}} \rho dv \tag{8.3-6}$$

This is the same as Equation (1.4-2). Let us now apply this equation to the pillbox-shaped volume in Figure 8.3-1(b). If we let the thickness Δx of the box become vanishingly small, and if we assume there is no surface charge at the boundary,

$$\int_{\text{closed surface}} \mathbf{D}\cdot\mathbf{n}dS = D_{\perp A}\Delta A - D_{\perp B}\Delta A = \int_{\text{volume}} \rho dv = 0 \tag{8.3-7}$$

Then

$$D_{\perp A} = D_{\perp B} \tag{8.3-8}$$

Thus the perpendicular component of electric flux density is continuous at a boundary.

(*b*) *Magnetic Fields*

Next, consider the boundary between regions of relative permeability μ_A and μ_B, as shown in Figure 8.3-2(a). The figure shows a single magnetic field line which passes through the boundary. A rectangle of dimensions Δx

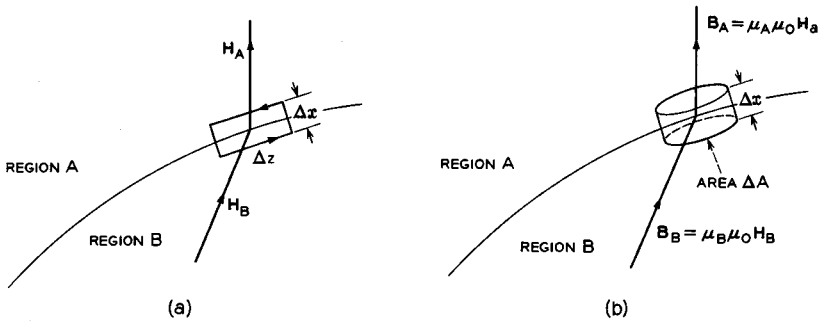

FIG. 8.3-2 Magnetic field vectors at a point on the boundary between two regions. Region A has permeability $\mu_A\mu_o$ and region B has permeability $\mu_B\mu_o$.

by Δz surrounds the point where the field line crosses the boundary and is centered about the boundary so that the rectangle lies in each region. We assume that $\mathbf{H}_A$ can be resolved into components $H_{\perp A}$ and $H_{\parallel A}$, perpendicular and parallel to the boundary. Similarly, $\mathbf{H}_B$ can be resolved into components $H_{\perp B}$ and $H_{\parallel B}$.

Let us evaluate Equation (8.1-15) for the region defined by the rectangle $\Delta x \Delta z$ in Figure 8.3-2(a). The equation can be written in the integral form

$$\int_{\text{surface}} (\nabla \times \mathbf{H}) \cdot \mathbf{n} dS = \int_{\text{surface}} (\mathbf{J} + j\omega \mathbf{D}) \cdot \mathbf{n} dS \tag{8.3-9}$$

Applying Stoke's theorem (see Appendix XII), we obtain

$$\oint_{\text{closed loop}} \mathbf{H} \cdot d\mathbf{l} = \int_{\text{surface}} (\mathbf{J} + j\omega \mathbf{D}) \cdot \mathbf{n} dS \tag{8.3-10}$$

If both Δx and Δz are very small, $\mathbf{H}$ in region A or B will be constant in magnitude and direction over the part of the rectangle included in the

region, and **J** and **D** will be uniform over the area of the rectangle. Let the average values of the components of **J** and **D** normal to the plane of the rectangle be J_n and D_n. Equation (8.3-10) can then be written as

$$\oint_{\text{closed loop}} \mathbf{H}\cdot d\mathbf{l} = H_{\|B}\Delta z + H_{\perp B}\frac{\Delta x}{2} + H_{\perp A}\frac{\Delta x}{2} - H_{\|A}\Delta z$$

$$-H_{\perp A}\frac{\Delta x}{2} - H_{\perp B}\frac{\Delta x}{2} = (J_n + j\omega D_n)\Delta x\Delta z \quad (8.3\text{-}11)$$

If we now let Δx approach zero, the right-hand side of the equation approaches zero, and the equation reduces to

$$H_{\|B}\Delta z - H_{\|A}\Delta z = 0 \quad (8.3\text{-}12)$$

or

$$H_{\|A} = H_{\|B} \quad (8.3\text{-}13)$$

Hence the tangential component of the magnetic field intensity vector is continuous at a boundary.

Finally, let us consider the normal components of magnetic field at the boundary. We shall start with Equation (8.1-17) in the integral form:

$$\int_{\text{volume}} \nabla\cdot\mathbf{B}dv = 0 \quad (8.3\text{-}14)$$

Using Gauss's theorem (Appendix XII) gives us

$$\int_{\text{closed surface}} \mathbf{B}\cdot\mathbf{n}dS = 0 \quad (8.3\text{-}15)$$

If this equation is applied to the pillbox-shaped volume shown in Figure 8.3-2(b) and if we let the thickness Δx of the volume become vanishingly small, we obtain

$$\int_{\text{closed surface}} \mathbf{B}\cdot\mathbf{n}dS = B_{\perp A}\Delta A - B_{\perp B}\Delta A = 0 \quad (8.3\text{-}16)$$

Hence

$$B_{\perp A} = B_{\perp B} \quad (8.3\text{-}17)$$

Thus the perpendicular component of magnetic flux density is continuous at a boundary.

In summary, at an infinitesimally thin boundary between two regions which have different permeability and permittivity, the tangential components of **E** and **H** are continuous, and the perpendicular components of **D** and **B** are continuous.

8.4 Ohm's Law and Skin Effect

(a) *Ohm's Law*

Ohm's Law is perhaps the first learned and most basic of the experimental laws of electricity. At low frequencies this law states that the ratio of voltage drop to current in a resistor is a constant. At microwave frequencies, the current density throughout a resistor or a conductor is usually not constant, and Ohm's Law is best stated in the form

$$\mathbf{J} = \sigma\mathbf{E} \tag{8.4-1}$$

where $\mathbf{J}$ is the current density, $\mathbf{E}$ is the electric field intensity, and σ is the conductivity of the medium.

This equation can be related to the more familiar form of Ohm's Law in the following way. Consider a conductor of length l and cross-sectional area A, as shown in Figure 8.4-1. A voltage V is applied over the length l, and a current density J flows parallel to the length l. We assume the current density is uniform over the cross section of the conductor. The electric field intensity within the conductor is of magnitude E. Then $J = \sigma E$, and the total current flowing in the conductor is given by

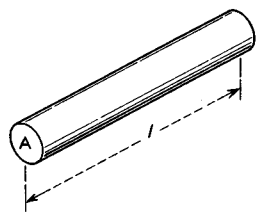

FIG. 8.4-1 A uniform cylindrical conductor of conductivity σ.

$$I = JA = \sigma EA = \sigma\frac{V}{l}A = \frac{V}{R} \tag{8.4-2}$$

or

$$V = IR \tag{8.4-3}$$

where $R = l/\sigma A$ is the resistance of the conductor over the length l. Equation (8.4-3) expresses the more familiar form of Ohm's Law.

(b) *Skin Effect*

Here we shall derive the distribution of current density in a semi-infinite conductor when an rf electric field is applied parallel to the surface of the conductor.[4] Figure 8.4-2 shows a portion of the conductor. We shall assume that the electric field is applied in the z direction only and that it does not vary in magnitude in the y and z directions. Let the electric field

[4]Reference 8a.

just outside the conductor be E_{zo}. From the discussion in Section 8.3, we know that this field will be continuous across the boundary between the conductor and free space, and hence that E_{zo} also will be the electric field intensity just inside the surface of the conductor. We shall first determine

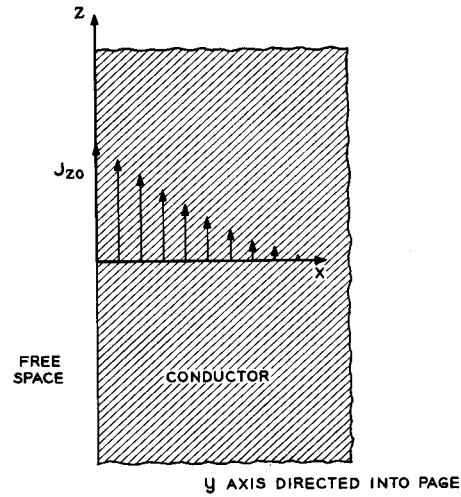

FIG. 8.4-2 Current flow near the surface of a conductor at microwave frequencies.

the variation of E_z with distance x into the conductor, and since $J_z = \sigma E_z$, we shall note that J_z varies in a similar manner with distance into the conductor.

Let us use Equations (8.1-18) and (8.1-19) to derive an equation for E_z within the conductor. Since $E_x = E_y = \partial E_z/\partial y = 0$, Equations (8.1-18) reduce to

$$H_x = H_z = 0 \tag{8.4-4}$$

and

$$j\omega\mu\mu_o H_y = \frac{\partial E_z}{\partial x} \tag{8.4-5}$$

We shall set $J_z = \sigma E_z$ and $J_x = J_y = 0$ in Equations (8.1-19). Then

$$\frac{\partial H_y}{\partial z} = 0 \tag{8.4-6}$$

and

$$\frac{\partial H_y}{\partial x} = (\sigma + j\omega\varepsilon\varepsilon_o)E_z \tag{8.4-7}$$

Substituting for H_y in Equation (8.4-7) from Equation (8.4-5), we obtain

$$\frac{\partial^2 E_z}{\partial x^2} = j\omega\mu\mu_o(\sigma + j\omega\varepsilon\varepsilon_o)E_z \tag{8.4-8}$$

Consideration of the actual values of σ, ω, and $\varepsilon\varepsilon_o$ for conductors at microwave frequencies shows that

$$\sigma \gg \omega\varepsilon\varepsilon_o \tag{8.4-9}$$

Hence to a good approximation

$$\frac{\partial^2 E_z}{\partial x^2} = j\omega\mu\mu_o\sigma E_z \tag{8.4-10}$$

This is the wave equation for an electric field in a conducting medium. The equation is analogous to Equation (8.1-26), which applies to electromagnetic waves in free space or in a dielectric medium. Equation (8.4-10) has the solution

$$E_z = E_{zo}\epsilon^{-(1+j)\sqrt{\omega\mu\mu_o\sigma/2}\,x} \tag{8.4-11}$$

Finally, substituting $J_z = \sigma E_z$ and $J_{zo} = \sigma E_{zo}$, we obtain

$$J_z = J_{zo}\epsilon^{-(1+j)\sqrt{\omega\mu\mu_o\sigma/2}\,x} \tag{8.4-12}$$

This equation shows that not only does the current density decay in magnitude away from the surface, but it also experiences a progressive phase shift. Although this relationship has been derived for a plane surface of infinite depth, it may be applied to curved surfaces of finite depth as long as the current decays in a distance small compared with the thickness and radius of curvature of the conductor.

It is convenient to write Equation (8.4-12) in the form

$$J_z = J_{zo}\epsilon^{-(1+j)x/\delta} \tag{8.4-13}$$

where

$$\delta = \frac{1}{\sqrt{\pi f\mu\mu_o\sigma}} \tag{8.4-14}$$

The length δ is known as the skin depth. The skin depth δ is a measure of the rate at which the current density decays into the metal. In a distance δ from the surface, the current density has dropped to $1/\epsilon$ of its value at the surface. This is a very rapid decay at microwave frequencies for most metals. Table 8.4-1 gives the number of skin depths in a 1.59 mm (1/16 inch) thick wall of several metals commonly used in microwave transmission

TABLE 8.4-1. NUMBER OF SKIN DEPTHS IN 1.59 MM THICKNESS WALLS OF VARIOUS MATERIALS

Metal	*Number at 3 Gc*	*Number at 9 Gc*
Silver	1352	2340
Copper	1318	2280
Gold	1106	1913
Molybdenum	726	1258
Nickel	583	1010
Stainless steel (nonmagnetic)	181	314

lines and electron tubes. This thickness is used for the wall of several standard size waveguides at microwave frequencies. Because the skin depth is so small at microwave frequencies, one normally assumes negligible currents exist on the outer surface of a waveguide or cavity. For example, at 3 Gc a copper waveguide of 1.59-mm wall thickness has current densities on the outer surface which are only 10^{-572} times the current density on the inner surface. Thus, in effect, perfect shielding is accomplished. Since the current density decays so rapidly with distance, the bulk of the metal in microwave conducting structures is not used to provide a path for current flow but rather is used for structural rigidity. It is an excellent approximation to visualize the wall currents in microwave structures as consisting solely of surface currents.

The imaginary part of the exponent in the right-hand side of Equation (8.4-11) gives the phase change of the electric field intensity as it propagates into the conductor. We see that the skin depth δ corresponds to $1/2\pi$ wavelengths of the type of wave propagation that takes place in the conductor.

One can use Equation (8.4-13) to determine the total ohmic power loss per unit surface area of the conductor for a given tangential component of magnetic field in free space just outside the conductor. The ohmic power loss in an element of volume having unit length parallel to the surface, unit width parallel to the surface, and thickness dx in the direction normal to the surface is $(1/2\sigma)\,|J_z|^2\,dx$. The total power loss per unit area of the surface is then

$$P_\square = \frac{1}{2\sigma}\int_0^\infty |J_z|^2 dx = \frac{\delta}{4\sigma}\,|J_{zo}|^2 \tag{8.4-15}$$

where we have substituted for J_z from Equation (8.4-13).

Often it is more convenient in using this equation to express J_{zo} in terms of the magnetic field in free space just outside the conductor. Within the

conductor we can rewrite Equation (8.3-10) in the form

$$\oint_{\text{closed loop}} \mathbf{H}\cdot d\mathbf{l} = \int_{\text{surface}} (\sigma + j\omega\varepsilon\varepsilon_o)\mathbf{E}\cdot\mathbf{n}dS \approx \int_{\text{surface}} \sigma\mathbf{E}\cdot\mathbf{n}dS$$

$$= \int_{\text{surface}} \mathbf{J}\cdot\mathbf{n}dS \tag{8.4-16}$$

where we have again made the approximation that $\sigma \gg \omega\varepsilon\varepsilon_o$ within the conductor. Figure 8.4-3 shows a cross-sectional view of the conductor near the

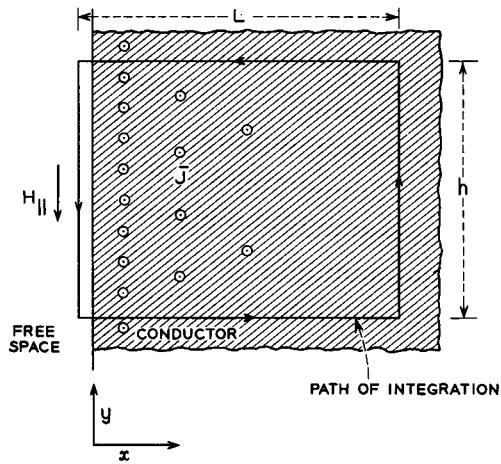

FIG. 8.4-3 Current flow in a conductor at microwave frequencies. The length L is much greater than δ. The component of magnetic field parallel to the path of integration is therefore zero along the right-hand side of the path of integration.

surface. The current flow J_z is assumed to be normal to the page and directed out of the page. Let us evaluate the left-hand side of Equation (8.4-16) for the path of integration shown in the figure. We assume that the length L is very large so that J_z is essentially zero at the right-hand side of the path. For symmetry reasons there is no net contribution to the line integral for a component of $\mathbf{H}$ parallel to the top and bottom sides of the path of integration (assuming h is infinitesimally short). Then

$$\oint_{\text{closed loop}} \mathbf{H}\cdot d\mathbf{l} = H_{||}h = \int_{\text{surface}} \mathbf{J}\cdot\mathbf{n}dS = J_{z_o}h\int_o^\infty \epsilon^{-(1+j)x/\delta}dx$$

$$= \frac{J_{z_o}h\delta}{1+j} \tag{8.4-17}$$

where $H_{||}$ is the magnetic field parallel to the surface just outside the conductor. Then

$$H_{||} = \frac{J_{z0}\delta}{1 + j} \tag{8.4-18}$$

Substituting into Equation (8.4-15), we obtain

$$P_{\square} = \frac{|H_{||}|^2}{2\sigma\delta} \tag{8.4-19}$$

This equation is most useful in the sense that ohmic losses in cavity or waveguide walls can be computed directly from the magnetic fields in the free space adjacent to the metal without resorting to calculations of the currents within the metal conductors themselves.

Equation (8.4-14) shows that δ is inversely proportional to the square root of the frequency. Hence, by Equation (8.4-19), the ohmic loss is proportional to the square root of the frequency, for a constant conductivity and for a given magnetic field at the surface.

(c) *The Perfect Conductor*

The concept of a perfect conductor is often used in the study of microwave components. In essence, this concept assumes, for purposes of solving for the fields in regions not containing metal, that the conductivity of the metal is infinite. Now, infinite conductivity implies that charges could travel instantaneously to neutralize any electric field which would tend to be set up within a conductor; thus the electric field within a perfect conductor is zero. Since the tangential component of electric field is continuous at the surface of the conductor, the tangential component of electric field outside the conductor must be zero adjacent to the surface. However, electric field lines can terminate on surface charges on the conductor, the field lines being perpendicular to the surface at the point of intersection. On the other hand, magnetic field lines cannot pass through a perfect conductor or terminate on it. Thus, there can only be a tangential component of magnetic field just outside a perfect conductor.

The errors involved in using the concept of a perfect conductor to find the external field distribution are of the same order of magnitude as the ratio of the skin depth to the other cavity or waveguide dimensions, and generally they may be considered to be negligible. Thus, for most purposes, the electromagnetic fields within a cavity or waveguide can be found under the assumption that the metal walls are perfect conductors. The fact that the conductor is imperfect affects only the power loss or attenuation, and this may be accounted for by using the concept of skin depth together with Equation (8.4-19).

8.5 Waveguides

In this section we shall discuss solutions of the wave equation for the case of electromagnetic wave propagation in a waveguide. Figure 8.5-1 shows an end view of a waveguide. We shall assume that the waveguide is of infinite length in the z direction and its cross-sectional dimensions remain constant with z. The walls of the waveguide are perfect conductors, so that the solutions we obtain must satisfy the boundary conditions that the tangential component of electric field and the normal component of magnetic field be zero at the conducting surfaces. It turns out that there are an infinite number of solutions to the wave equation which satisfy these boundary conditions. These solutions are known as *modes of propagation.* This is analogous to the infinite number of possible modes of vibration for a vibrating string. Which modes are vibrated depend on how the string is plucked. In the waveguide, the manner and frequency of excitation at the input determine which modes are excited.

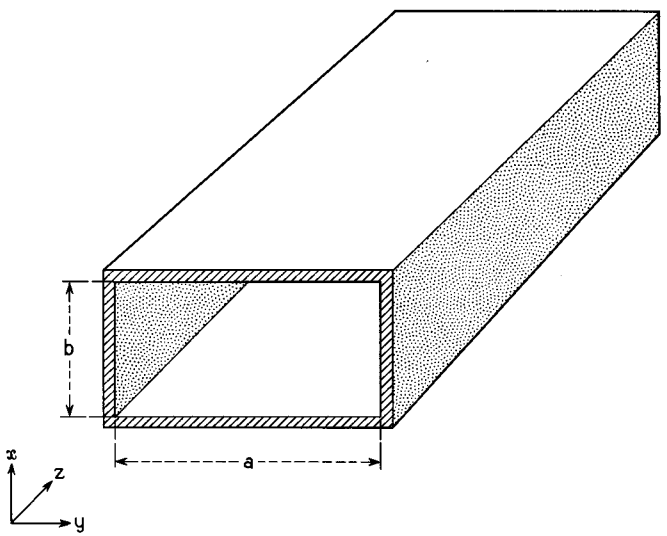

FIG. 8.5-1 Rectangular waveguide.

The infinite number of waveguide modes of propagation can be divided into two classes. Modes with E_z equal to zero are known as transverse electric modes or TE modes. Modes with H_z equal to zero are known as transverse magnetic modes or TM modes. As long as the waveguide is

uniformly filled with dielectric (including air or vacuum) the solutions fall into one or the other of these two classes.[5]

(*a*) TE *Modes*

The solution for the TE modes can be obtained as follows. The wave equations, Equations (8.1-26) and (8.1-27), are vector equations and hence are satisfied by each component of the electric and magnetic fields. Thus the z component of magnetic field satisfies the equation

$$\nabla^2 H_z + k^2 H_z = 0 \tag{8.5-1}$$

where $k^2 = \omega^2 \mu\mu_o \varepsilon\varepsilon_o$. Expanding the Laplacian, we obtain

$$\frac{\partial^2 H_z}{\partial x^2} + \frac{\partial^2 H_z}{\partial y^2} + \frac{\partial^2 H_z}{\partial z^2} + k^2 H_z = 0 \tag{8.5-2}$$

A particular solution to this equation may be obtained by the method of separation of variables as

$$H_z = A \cos \frac{m\pi y}{a} \cos \frac{n\pi x}{b} \epsilon^{-j\beta z} \tag{8.5-3}$$

where m and n are arbitrary integers. We shall see later that this solution meets the boundary conditions imposed by the waveguide walls. Substituting Equation (8.5-3) into Equation (8.5-2), we find that the following relationship must be satisfied for Equation (8.5-3) to be a solution:

$$\beta^2 + \left(\frac{m\pi}{a}\right)^2 + \left(\frac{n\pi}{b}\right)^2 = k^2 = \omega^2 \mu\mu_o \varepsilon\varepsilon_o = \frac{\omega^2}{c^2} \tag{8.5-4}$$

The presence of the integers m and n in this equation indicates that there are an infinite number of solutions corresponding to an infinite number of modes of propagation.

If the variation of the magnetic field with time is included in Equation (8.5-3), the equation becomes

$$\begin{aligned} \mathcal{H}_z &= \text{Re } A \cos \frac{m\pi y}{a} \cos \frac{n\pi x}{b} \epsilon^{j(\omega t - \beta z)} \\ &= A \cos \frac{m\pi y}{a} \cos \frac{n\pi x}{b} \cos (\omega t - \beta z) \end{aligned} \tag{8.5-5}$$

We see that the wave travels in the z direction with a phase velocity given by

$$v_p = \frac{\omega}{\beta} \tag{8.5-6}$$

---

[5]Reference 8.3.

where β is determined by Equation (8.5-4) and is a characteristic of the particular mode of propagation.

The other components of the fields in the waveguide can be obtained from Equation (8.5-3) by means of Equations (8.1-18) and (8.1-19). Let us first note that (1) E_z is zero, and (2) all field quantities will vary with z as $\epsilon^{-j\beta z}$, so that differentiating with respect to z is equivalent to multiplying by $-j\beta$. We shall assume that the waveguide is filled with air, so that to a good approximation $\mu = \varepsilon = 1$. Equations (8.1-18) then give

$$j\beta E_y = -j\omega\mu_o H_x \tag{8.5-7}$$

and

$$j\beta E_x = j\omega\mu_o H_y \tag{8.5-8}$$

From Equations (8.1-19) we obtain

$$-j\beta H_x - \frac{\partial H_z}{\partial x} = j\omega\varepsilon_o E_y \tag{8.5-9}$$

and

$$\frac{\partial H_z}{\partial y} + j\beta H_y = j\omega\varepsilon_o E_x \tag{8.5-10}$$

Finally, combining Equations (8.5-7) and (8.5-9) as well as Equation (8.5-3) gives

$$E_y = \frac{-j\omega\mu_o}{k^2 - \beta^2}\frac{n\pi}{b}A \cos\frac{m\pi y}{a}\sin\frac{n\pi x}{b}\epsilon^{-j\beta z} \tag{8.5-11}$$

and

$$H_x = \frac{j\beta}{k^2 - \beta^2}\frac{n\pi}{b}A \cos\frac{m\pi y}{a}\sin\frac{n\pi x}{b}\epsilon^{-j\beta z} \tag{8.5-12}$$

Combining Equations (8.5-8), (8.5-10), and (8.5-3) gives

$$E_x = \frac{j\omega\mu_o}{k^2 - \beta^2}\frac{m\pi}{a}A \sin\frac{m\pi y}{a}\cos\frac{n\pi x}{b}\epsilon^{-j\beta z} \tag{8.5-13}$$

and

$$H_y = \frac{j\beta}{k^2 - \beta^2}\frac{m\pi}{a}A \sin\frac{m\pi y}{a}\cos\frac{n\pi x}{b}\epsilon^{-j\beta z} \tag{8.5-14}$$

Examination of Equations (8.5-11) through (8.5-14) shows that H_x is zero when $x = 0$ and when $x = b$, and $H_y = 0$ when $y = 0$ and when $y = a$. Similarly, $E_x = 0$ when $y = 0$ and when $y = a$, and $E_y = 0$ when $x = 0$ and when $x = b$. Thus the normal component of **H** and the tangential component of **E** are zero at the inside walls of the waveguide. The field

solutions given by Equations (8.5-3) and (8.5-11) through (8.5-14) therefore satisfy the wave equation and the boundary conditions imposed by the waveguide.

From Equations (8.5-7) and (8.5-8) we note that

$$\frac{E_x}{H_y} = -\frac{E_y}{H_x} = \frac{\omega\mu_o}{\beta} \tag{8.5-15}$$

showing that the perpendicular components of **E** and **H** are constant through the cross section of the waveguide.

In the introductory part of this chapter, we described the dominant TE mode, that is the TE mode with the lowest cutoff frequency. This is the TE_{10} mode ($m = 1$, $n = 0$). The field components for this mode are

$$E_x = \frac{j\omega\mu_o aA}{\pi} \sin\frac{\pi y}{a}\epsilon^{-j\beta z} \tag{8.5-16}$$

$$H_y = \frac{j\beta aA}{\pi} \sin\frac{\pi y}{a}\epsilon^{-j\beta z} \tag{8.5-17}$$

$$H_z = A \cos\frac{\pi y}{a}\epsilon^{-j\beta z} \tag{8.5-18}$$

and

$$E_y = E_z = H_x = 0 \tag{8.5-19}$$

The field configuration for this mode is shown in Figure 8-5.

Setting $m = 1$, $n = 0$ in Equation (8.5-4) gives

$$\beta^2 + \left(\frac{\pi}{a}\right)^2 = k^2 = \frac{\omega^2}{c^2} = \left(\frac{2\pi}{\lambda_o}\right)^2 \tag{8.5-20}$$

or

$$\beta^2 = \left(\frac{2\pi}{\lambda_o}\right)^2\left(1 - \frac{\lambda_o^2}{\lambda_c^2}\right) \tag{8.5-21}$$

where we have set $\lambda_o = 2\pi c/\omega$, the free-space wavelength of a wave of radian frequency ω, and $\lambda_c = 2a$, as in the introductory part of this chapter. The phase velocity for the TE_{10} mode then becomes

$$v_p = \frac{\omega}{\beta} = \frac{\omega\lambda_o}{2\pi\sqrt{1 - \lambda_o^2/\lambda_c^2}} = \frac{c}{\sqrt{1 - \lambda_o^2/\lambda_c^2}} \tag{8.5-22}$$

as in Equation (8-5). Similarly

$$\lambda_z = \frac{2\pi}{\beta} = \frac{\lambda_o}{\sqrt{1 - \lambda_o^2/\lambda_c^2}} \tag{8.5-23}$$

Next let us consider the group velocity v_g. This is equal to the time average power flow in the waveguide divided by the energy stored per unit

length in the z direction. From Equation (8.2-11), the time average power flow for the TE_{10} mode is given by

$$\text{time average power flow} = \int_{\substack{\text{area of} \\ \text{waveguide}}} (\text{time average of } |\,\mathbf{S}\,|)dxdy$$

$$= \frac{\beta\omega\mu_o a^3 b A^2}{4\pi^2} \tag{8.5-24}$$

where (time average of $|\,\mathbf{S}\,|$) = (time average of $|\,\mathcal{E} \times \mathcal{H}\,|$) = $\frac{1}{2}\,|\,E_x H_y\,|$, and we have substituted for E_x and H_y from Equations (8.5-16) and (8.5-17) From Equations (8.2-2), (8.2-7), and Equation (6) of Appendix XIV, the average energy stored per unit length in the z direction is given by

energy stored per unit length

$$= \frac{1}{\lambda_z}\int_{x=0}^{b}\int_{y=0}^{a}\int_{z=0}^{\lambda_z}\frac{1}{4}(\varepsilon_o\,|\,E_x\,|^2 + \mu_o\,|\,H_y\,|^2 + \mu_o\,|\,H_z\,|^2)dxdydz = \frac{\omega^2\mu_o a^3 b A^2}{4\pi^2 c^2} \tag{8.5-25}$$

Then

$$v_g = \frac{\text{time average power flow}}{\text{energy stored per unit length}} = \frac{\beta c^2}{\omega} = c\sqrt{1 - \lambda_o^2/\lambda_c^2} \tag{8.5-26}$$

as in Equation 8-6. Some further discussion of the group velocity is given in Appendix XIII where it is shown that

$$v_g = \frac{\partial\omega}{\partial\beta} \tag{8.5-27}$$

From Equation (8.5-4) it is evident that $\beta\partial\beta = \omega\partial\omega/c^2$, and hence

$$v_p v_g = c^2 \tag{8.5-28}$$

Substituting for v_p from Equation (8.5-22) in this expression, we obtain $v_g = c\sqrt{1 - \lambda_o^2/\lambda_c^2}$, as in Equation (8.5-26).

The *characteristic impedance*[6] of the waveguide is defined in terms of the time average power flow and a "voltage" at the center of the waveguide given by the integral $\int_0^b E_x dx$, where E_x is evaluated at $y = a/2$. From Equation (8.5-16), the mean-square value of this voltage is

$$\begin{matrix}\text{mean-square "voltage"} \\ \text{at center of waveguide}\end{matrix} = \frac{\omega^2\mu_o^2 a^2 A^2 b^2}{2\pi^2} \tag{8.5-29}$$

---

[6]This definition is not unique. Two other definitions for waveguide impedance are also used. See Reference 8b, pp. 36, 37.

The characteristic impedance for the TE_{10} mode is then given by

$$Z_o = \frac{\text{mean-square voltage}}{\text{time average power flow}} = \frac{2b}{a}\frac{\sqrt{\mu_o/\varepsilon_o}}{\sqrt{1-\lambda_o^2/\lambda_c^2}} = \frac{754b}{a\sqrt{1-\lambda_o^2/\lambda_c^2}} \text{ ohms} \tag{8.5-30}$$

where we have substituted from Equation (8.5-24) for the time average power flow.

Let us plot Equation (8.5-4) as ω vs. β. We obtain the family of hyperbolas shown in Figure 8.5-2. Note that each mode has a cutoff frequency given by $\beta = 0$ in Equation (8.5-4):

$$\omega_{\text{cutoff}} = c\sqrt{\left(\frac{m\pi}{a}\right)^2 + \left(\frac{n\pi}{b}\right)^2} \tag{8.5-31}$$

Furthermore, each curve is asymptotic to the straight line

$$\omega = \beta c \tag{8.5-32}$$

This straight line has a slope equal to c, the velocity of light. A simple geometric construction enables us to obtain the phase velocity corresponding to any frequency for any mode. Suppose we want to know the phase velocity corresponding to propagation in the TE_{01} mode at a radian frequency ω_1. The slope of a line drawn from the origin to a point on the ω-β

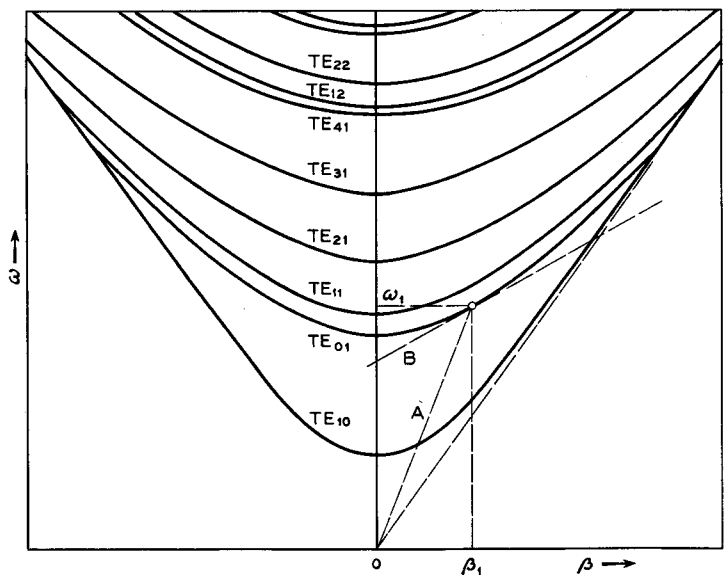

FIG. 8.5-2 ω-β diagram for the TE modes in a rectangular waveguide. All the curves are asymptotic to lines through the origin with slopes equal in magnitude to the velocity of light. $a/b = 2.3$.

curve for the correct mode and frequency (line A in Figure 8.5-2) gives the phase velocity, according to Equation (8.5-22). Note that the phase velocity for all propagating frequencies and all modes is greater than the velocity of light. If the waveguide were filled with a dielectric of relative dielectric constant ε, the asymptote would correspond to $c = 1/\sqrt{\varepsilon\varepsilon_o\mu_o}$. The fact that the phase velocity is greater than the velocity of light is a universal property of waveguides of this type, having transverse dimensions invariant with axial position.

The group velocity $v_g = \partial\omega/\partial\beta$ is equal to the slope of a line tangent to the ω-β curve at the operating frequency (line B in Figure 8.5-2). It is evident that the group velocity is always less than the velocity of light.

(*b*) TM *Modes*

So far we have considered only the transverse electric or TE modes. We shall now consider the equivalent relationships for the transverse magnetic or TM modes.

We may begin consideration of the TM modes by considering the z component of Equation (8.1-26).

$$\nabla^2 E_z + k^2 E_z = 0 \tag{8.5-33}$$

A particular solution to this equation is given by

$$E_z = A \sin \frac{m\pi y}{a} \sin \frac{n\pi x}{b} \epsilon^{-j\beta z} \tag{8.5-34}$$

where m and n are integers. When this solution is substituted back into Equation (8.5-23), we find that

$$\beta^2 + \left(\frac{m\pi}{a}\right)^2 + \left(\frac{n\pi}{b}\right)^2 = k^2 = \omega^2\mu\mu_o\varepsilon\varepsilon_o \tag{8.5-35}$$

as in the case of TE modes (Equation (8.5-4)).

The other field components may be obtained from Equation (8.5-34) by application of Equations (8.1-18) and (8.1-19), in which case we set $H_z = 0$. Thus we obtain

$$H_x = \frac{j\omega\varepsilon_o}{k^2 - \beta^2} \frac{m\pi}{a} A \cos \frac{m\pi y}{a} \sin \frac{n\pi x}{b} \epsilon^{-j\beta z} \tag{8.5-36}$$

$$H_y = -\frac{j\omega\varepsilon_o}{k^2 - \beta^2} \frac{n\pi}{b} A \sin \frac{m\pi y}{a} \cos \frac{n\pi x}{b} \epsilon^{-j\beta z} \tag{8.5-37}$$

$$E_x = -\frac{j\omega\beta}{k^2 - \beta^2} \frac{n\pi}{b} A \sin \frac{m\pi y}{a} \cos \frac{n\pi x}{b} \epsilon^{-j\beta z} \tag{8.5-38}$$

$$E_y = -\frac{j\beta}{k^2 - \beta^2} \frac{m\pi}{a} A \cos \frac{m\pi y}{a} \sin \frac{n\pi x}{b} \epsilon^{-j\beta z} \tag{8.5-39}$$

It is easily shown that these field components satisfy the boundary condi-

tions imposed by the waveguide, and hence these are the field components associated with transverse magnetic waves. Figure 8.5-3 shows the field pattern for the TM_{11} mode ($m = n = 1$).

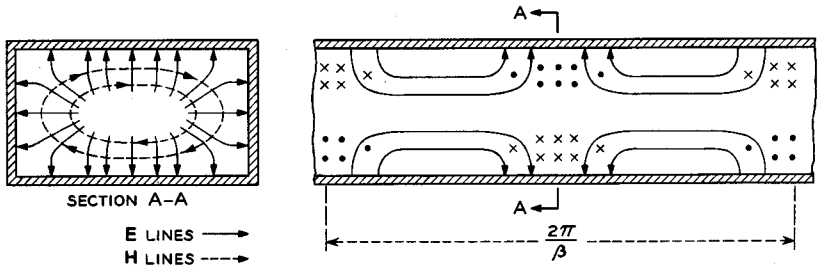

FIG. 8.5-3 TM_{11} mode in a rectangular waveguide.

A complete ω-β diagram for both the TE and TM modes is shown in Figure 8.5-4. All of the TM modes are degenerate; that is, a TE mode has the same ω-β curve. The two lowest modes are TE modes and have no TM counterpart. Rectangular waveguide is normally operated in the mode of lowest cutoff frequency, the TE_{10} mode.

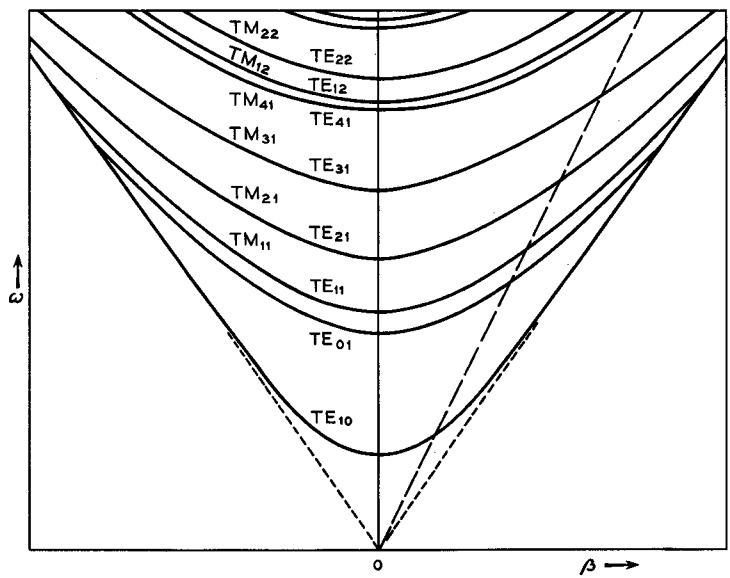

FIG. 8.5-4 Complete ω-β diagram for a rectangular waveguide. All the curves are asymptotic to the velocity of light lines. $a/b = 2.3$.

The relationships of power flow, group velocity, and phase velocity are the same for TM as for TE modes. If, for instance, we draw a straight line from the origin, as shown in Figure 8.5-4, then at the frequencies of intersection on each mode branch the phase velocities are all the same; correspondingly, by Equation (8.5-28), the group velocities are also identical at these points.

We have not considered any losses in the above discussion. Losses may be taken into account by allowing the propagation constant β to be complex, so that the wave is attenuated in the z direction. In this manner, we can allow both for resistive losses in the walls and also dielectric losses if the guide contains dielectric.

Transmission line theory may be applied directly to waveguides. For instance, a quarter wavelength away from a short circuit one sees an open circuit. Of course, in the case of a waveguide, a wavelength is no longer equal to a free space wavelength c/f. Rather it is a guide wavelength, given by $\lambda_z = 2\pi/\beta$, and β is obtained from the ω-β curve; λ_z is thus a function of frequency and of the mode of propagation.

No mention has yet been made of coupling energy in or out of a waveguide. One common method of coupling between a coaxial line and a waveguide is shown in Figure 8.5-5. The center conductor of a coaxial line is brought down through the broad wall of the waveguide. The center conductor acts like an antenna to radiate energy into the waveguide. A short is placed in the waveguide a quarter wavelength to the left of the probe causing the region to the left of the probe to look like an open circuit at the probe. Hence, resultant power flow is to the right. At the receiving end of the waveguide, a similar transition may be used to couple energy back into a coaxial line.

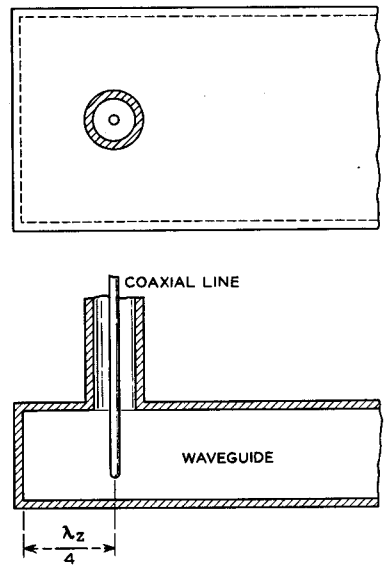

FIG. 8.5-5 Coaxial line to waveguide transition.

8.6 Cavity Resonators

In the introductory section of this chapter, we looked at cavity resonators from the point of view of an evolution from a simple L-C circuit. With the

discussion of waveguides behind us, we can now look at cavity resonators from a different point of view.

Let us consider the electric field solutions for the TE_{10} mode in a rectangular waveguide. From Equations (8.5-16) and (8.5-19),

$$E_x = B \sin \frac{\pi y}{a} \epsilon^{-j\beta z} \tag{8.6-1}$$

$$E_y = E_z = 0 \tag{8.6-2}$$

Now this solution corresponds to a wave traveling in the positive z direction. There is an equally valid solution corresponding to propagation in the negative z direction:

$$E_x = C \sin \frac{\pi y}{a} \epsilon^{+j\beta z} \tag{8.6-3}$$

$$E_y = E_z = 0 \tag{8.6-4}$$

where β is taken to be positive in both Equations (8.6-1) and (8.6-3). Physically, the wave traveling in the negative z direction could be set up by an obstacle in a waveguide which reflects part of the outgoing energy back toward the source. The general solution is thus given by the superposition of the above two waves, resulting in

$$E_x = (B\epsilon^{-j\beta z} + C\epsilon^{+j\beta z}) \sin \frac{\pi y}{a} \tag{8.6-5}$$

$$E_y = E_z = 0 \tag{8.6-6}$$

Now, we can make a rectangular cavity resonator out of a rectangular waveguide simply by placing walls perpendicular to the z axis at $z = 0$ and $z = L$. Equation (8.6-5) must then satisfy the additional boundary condition of being zero at the added walls. Setting E_x to zero at $z = 0$ gives us

$$0 = B + C \tag{8.6-7}$$

so that Equation (8.6-5) may be written

$$E_x = 2jC \sin \beta z \sin \frac{\pi y}{a} \tag{8.6-8}$$

The additional boundary condition at $z = L$ is satisfied for

$$\beta = \frac{p\pi}{L} \tag{8.6-9}$$

where p is an integer. Since $\lambda_z = 2\pi/\beta$, this states that the cavity must be an integral number of half guide wavelengths long.

Using Equation (8.4-30) and setting $m = 1$ and $n = 0$ for the case of the

TE_{10} mode, we obtain an expression for the resonant frequencies of the cavity:

$$\omega_p = c\sqrt{\left(\frac{p\pi}{L}\right)^2 + \left(\frac{\pi}{a}\right)^2}, \qquad p = 1,2,3 \ldots \tag{8.6-10}$$

A sketch of the lowest frequency, or $p = 1$, mode of oscillation is shown in Figure 8.6-1 for the case in which $L = a$. In a cavity at resonance, the

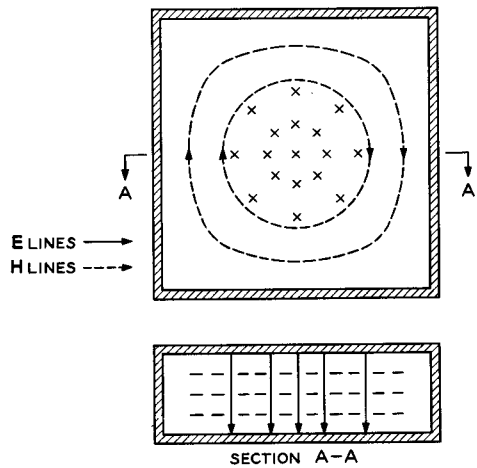

FIG. 8.6-1 Field patterns for the dominant mode of a rectangular cavity resonator.

electric and magnetic lines are 90 degrees out of time phase. The stored energy oscillates back and forth between the two kinds of fields. Unlike the waveguide fields, the resonator fields remain fixed in space, varying sinusoidally with time uniformly throughout the cavity.

This resonator and its field patterns may be compared with the reentrant cavity of Figure 8-1. One might have anticipated that the patterns of Figure 8.6-1 would occur when the heights of the posts in Figure 8-1(d) are reduced to zero.

A field analysis such as we have just carried out also enables one to obtain the resonant frequencies of all the higher-order modes. These higher-order modes are usually of interest not because of their utility but rather because of the trouble they can cause. For instance, in a magnetron, higher-order modes may give rise to undesirable output signals.

Resonant cavities of the type considered here are useful as microwave circuit elements. In essence, they are low-loss resonant circuits, and they may be coupled together in various ways to achieve filter-type characteristics.

As an example of a rectangular cavity resonator, let us consider a resonator of the general shape shown in Figure 8.6-1. If we assume the base to be square, Equation (8.6-10) indicates the cavity will resonate in the TE_{101} mode ($m = 1, n = 0, p = 1$) at a frequency of 3000 Mc for $a = L = 7.07$ cm. The largest dimension of the re-entrant cavity of Figure 8-2 resonant at the same frequency was only 1.85 cm. Thus the effect of re-entrancy in a cavity is seen to be a decrease in overall size for the same resonant frequency. Further analysis reveals that this decrease in size is obtained at the expense of increased losses for the same stored energy in the two types of cavity.

8.7 Slow-Wave Structures

We have seen in Section 8.5 that wave propagation in ordinary waveguides is characterized by a phase velocity which is greater than the velocity of light. The phase velocity is the velocity with which an observer would have to move so as to remain always in the same phase of the wave.

In the operation of traveling-wave and magnetron type devices, the electron beam must keep in step (or nearly in step) with a propagating wave Since electrons can be accelerated only to velocities which are less than the velocity of light, we must look for microwave circuits or structures capable of propagating waves with phase velocities less than the velocity of light.

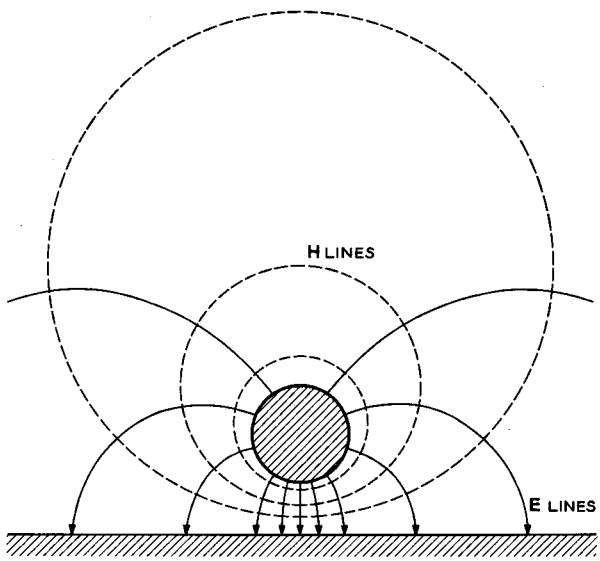

FIG. 8.7-1 Transmission line composed of a single wire above a ground plane.

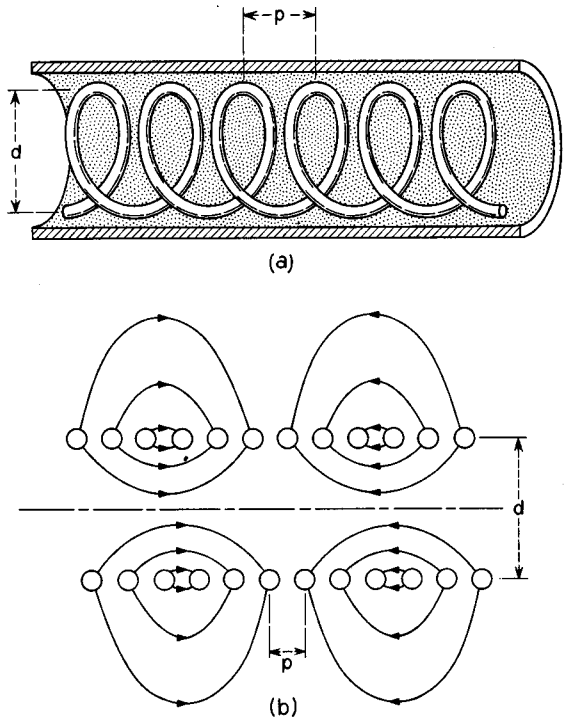

FIG. 8.7-2 The helix slow-wave structure. (a) Helical coil within a concentric conducting cylinder. This slow-wave circuit is obtained by wrapping the single-wire-above-ground into a helix, with the ground plane becoming the surrounding cylinder. (b) Electric field lines for a helix in free space.

For reasons that will become clearer in later chapters, ordinary waveguides partially or completely filled with dielectric are not satisfactory solutions to this problem. Instead, the solution will be found in a whole new class of structures appropriately called slow-wave structures or slow-wave circuits.

A simple, yet highly useful, slow-wave circuit can be demonstrated easily. Consider first a transmission line consisting of a single wire above a ground plane as shown in Figure 8.7-1. The propagation characteristics of such a line are well known.[7] An oppositely charged image of the round conductor may be constructed within the ground plane, whereby the behavior of the single-wire-above-ground line becomes identical with the common two-wire line. This line propagates a TEM mode in a direction parallel to the axis of

[7]Reference 8.2.

the wire at the velocity of light. The TEM designation means that both the electric and magnetic field lines lie entirely in the transverse plane.

Now it is intuitively obvious that gradual bends or twists of the wire above the ground plane, keeping the spacing from wire to ground constant, will have only a minor effect on propagation characteristics of the line. The field lines will faithfully follow the wire, despite such bends. Thus we can imagine the line distorted into the helical coil shown in Figure 8.7-2(a). The requirement that the spacing from wire to ground remain constant is met by having the ground plane become a cylinder enclosing the coil. If the spacing from wire to cylinder is much less than the cylinder diameter and much less than the spacing between turns, the electric field lines from each wire will terminate almost entirely on the adjacent cylinder surface, and the field pattern will be similar to that of Figure 8.7-1.

Since the wave follows the wire at very nearly the velocity of light, the resultant velocity along the axis of the cylinder must be less than the velocity of light. Consequently, an electron can be shot along the cylinder axis at a velocity which enables it to keep in step with the wave. The velocity at which the "in step" electron moves is the phase velocity of the slow-wave circuit. From geometrical considerations, this phase velocity is easily shown to be approximately given by

$$v_p = c\frac{p}{\sqrt{p^2 + (\pi d)^2}} \tag{8.7-1}$$

where d and p are the helix diameter and pitch, respectively.

Helices are commonly used as slow-wave circuits in low and medium power traveling-wave tubes. However, generally they are employed without the attendant conducting cylinder surrounding the helix. This causes some quantitative changes in the physical picture presented above, but the basic nature of the slowing process is unchanged. Figure 8.7-2(b) shows the approximate shape of the electric field lines when no outer cylinder is present. For the particular case chosen in the figure, the free-space wavelength of the signal is approximately equal to the length of wire in twelve turns of the helix.

For a structure to be a slow-wave circuit, it is necessary that it possess physical periodicity in the axial direction. That is, there is a finite length, called the period, by which the infinitely long structure must be translated in the axial direction so that one obtains the same structure back again, point for point. In the case of the helical circuit of Figure 8.7-2, for instance, a translation back or forth through a distance of one pitch length results in identically the same structure again. Thus, the period of this helical slow-wave structure is the same as its pitch.

Only periodic structures can propagate slow waves when filled with air or vacuum. It can be shown that smooth, air- or vacuum-filled, nonperiodic structures such as the waveguides of Section 8.4 propagate fast waves only.

(a) *Floquet's Theorem*

Since slow-wave structures are necessarily periodic structures,[8] let us examine some general theorems concerning the solutions of Maxwell's Equations and the relations between phase velocity, group velocity, stored energy, and power flow in periodic structures.

Floquet's Theorem concerns the nature of the single-frequency solutions for the electromagnetic fields obtained from Maxwell's Equations. It may be stated as follows for a periodic structure consisting of identical cells of periodic length L placed end to end.

> The steady-state solutions for the electromagnetic fields of a single propagating mode in a periodic structure have the property that fields in adjacent cells are related by a multiplicative complex constant, this constant being the same for all pairs of adjacent cells.

Mathematically the theorem may be stated as

$$\mathbf{E}(x,y,z - L) = \Gamma\mathbf{E}(x,y,z) \tag{8.7-2}$$

where L is the length of one period of the structure, and Γ is a complex constant. The direction of propagation is along the z axis, as before. The same expression can be written with $\mathbf{E}$ replaced by $\mathbf{H}$.

The proof of Floquet's Theorem may be obtained by use of the uniqueness theorem[9] of electromagnetic theory which states that the field solutions in two identical microwave structures, operating at the same frequency, can differ only by a complex multiplicative constant, corresponding physically to two different levels of excitation. An analogous situation occurs in ordinary circuit theory where two identical circuits are excited by two different sources at the same frequency. The corresponding phasor currents in the two circuits can differ only by a complex constant, equal to the ratio of the phasors representing the two sources.

Consider the infinitely long periodic structures shown schematically in Figure 8.7-3(a). Each cell is numbered for identification purposes. Assume that the solutions for the electromagnetic fields for a wave propagating to the right have been obtained. Thus, the electric field in cell n may be designated

$$\mathbf{E}_{an}$$

---

[8]Reference 8f.
[9]Reference 8c, pp. 486–488.

where the first subscript indicates that the solution pertains to the circuit in Figure 8.7-3(a), and the second subscript identifies the cell number.

Now let us consider a second structure obtained from the first by a linear translation in the axial direction of one periodic length as shown in

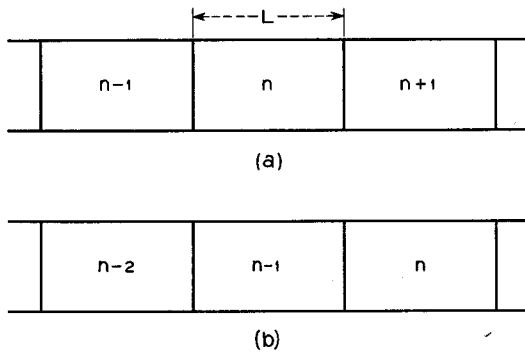

FIG. 8.7-3 Infinitely long periodic structures having identical boundary conditions. (a) The original structure. (b) Structure obtained from the original structure by a linear translation of one period in the axial direction.

Figure 8.7-3(b). Because of the translational symmetry, the new structure will appear identical to the old structure. The uniqueness theorem requires that the fields of structure b be identical to those of structure a, except for a constant complex multiplier. That is,

$$\begin{aligned} \mathbf{E}_{b(n-1)} &= \Gamma \mathbf{E}_{an} \\ \mathbf{E}_{bn} &= \Gamma \mathbf{E}_{a(n+1)}, \text{ etc.} \end{aligned} \tag{8.7-3}$$

Now we identify structure b by its true nature; it is, after all, merely a translated version of structure a so that the field pattern in structure b is the same as in structure a but translated one period to the right.

$$\begin{aligned} \mathbf{E}_{b(n-1)} &= \mathbf{E}_{a(n-1)} \\ \mathbf{E}_{bn} &= \mathbf{E}_{an}, \text{ etc.} \end{aligned} \tag{8.7-4}$$

Combining Equations (8.7-3) and (8.7-4), we get

$$\begin{aligned} \mathbf{E}_{a(n-1)} &= \Gamma \mathbf{E}_{an} \\ \mathbf{E}_{an} &= \Gamma \mathbf{E}_{a(n+1)}, \text{ etc.} \end{aligned} \tag{8.7-5}$$

This proves the theorem, since n is, of course, arbitrary.

This simple and highly useful theorem is analogous to theorems concerned with wave propagation in other types of periodic ensembles. For instance, the currents and voltages in an infinite chain of identical filter sections are

governed by the same basic rule; that is, the currents and voltages of one section are equal to the corresponding quantities in the preceding section multiplied by a complex constant. This analogy is often put to use when a microwave periodic structure is represented by an equivalent circuit consisting of such a chain of filter sections.[10]

Let us now rewrite the complex constant Γ in Equation (8.7-2) using the defining relationship

$$\Gamma \equiv \epsilon^{j\beta_o L} \tag{8.7-6}$$

so that Equation (8.7-2) becomes

$$\mathbf{E}(x,y,z - L) = \epsilon^{j\beta_o L}\mathbf{E}(x,y,z) \tag{8.7-7}$$

Now, β_o could in general be complex. If it were a pure real quantity, it is clear that Equation (8.7-7) implies only a phase shift from one cell to the next. A negative imaginary part to β_o would imply a decay in the strength of the fields with distance along the structure, corresponding to ohmic losses. For simplicity, let us assume a lossless structure, so that β_o is real. Our results can be generalized later by allowing β_o to be complex, if we wish to take losses into account.

Now we shall postulate that the solution to Maxwell's Equations in a periodic structure can be written in the following form

$$\mathbf{E}(x,y,z) = \mathbf{E}_p(x,y,z)\epsilon^{-j\beta_o z} \tag{8.7-8}$$

where $\mathbf{E}_p(x,y,z)$ is a periodic function of z with period L. A similar expression holds when $\mathbf{E}$ is replaced by $\mathbf{H}$. Equation (8.7-8) can be proven to be the solution if two conditions are fulfilled. First, it must satisfy the wave equation for the electric field, Equation (8.1-26) and the proper boundary conditions; and second, it must satisfy Floquet's Theorem, Equation (8.7-2). Let us first show that the latter condition is satisfied.

Equation (8.7-8) can be rewritten with z replaced by $z - L$.

$$\mathbf{E}(x,y,z - L) = \mathbf{E}_p(x,y,z - L)\epsilon^{-j\beta_o(z-L)} \tag{8.7-9}$$

Since $\mathbf{E}_p$ is a periodic function with period L,

$$\mathbf{E}_p(x,y,z - L) = \mathbf{E}_p(x,y,z) \tag{8.7-10}$$

so that Equation (8.7-9) becomes

$$\mathbf{E}(x,y,z - L) = \mathbf{E}_p(x,y,z)\epsilon^{-j\beta_o z}\epsilon^{+j\beta_o L} \tag{8.7-11}$$

Equation (8.7-8) may be used in the right-hand side of this equation, obtaining

$$\mathbf{E}(x,y,z - L) = \mathbf{E}(x,y,z)\epsilon^{j\beta_o L} \tag{8.7-12}$$

---

[10]Reference 8h, Chapter 4.

But this expression is the mathematical statement of Floquet's Theorem, Equation (8.7-7). Therefore, Equation (8.7-8) does indeed satisfy Floquet's Theorem.

The requirement that the right-hand side of Equation (8.7-8) should satisfy the wave equation will be applied later after we write Equation (8.7-8) in a more convenient form. Since $\mathbf{E}_p(x,y,z)$ is periodic in z with period L, we can express it by means of a Fourier series:

$$\mathbf{E}_p(x,y,z) = \sum_{-\infty}^{\infty} \mathbf{E}_n(x,y)\epsilon^{-j(2\pi n/L)z} \tag{8.7-13}$$

This equation is a vector equation, and it is merely a shorthand way of writing three separate equations, one for each vector component. The quantities $\mathbf{E}_n$ in the Fourier sum are the usual Fourier coefficients, except that they are functions of the transverse coordinates x and y. This may seem strange at first to one who is more familiar with the usual Fourier series in time, where the Fourier coefficients are constants. From this more conventional point of view, Equation (8.7-13) actually represents an infinite number of Fourier series, one for each choice of x and y.

Using Equation (8.7-13), the solution for a propagating wave in a periodic structure, Equation (8.7-8) can be written

$$\mathbf{E}(x,y,z) = \sum_{-\infty}^{\infty} \mathbf{E}_n(x,y)\epsilon^{-j(\beta_o+2\pi n/L)z} \tag{8.7-14}$$

Defining

$$\beta_n = \beta_o + \frac{2\pi n}{L} \tag{8.7-15}$$

we have

$$\mathbf{E}(x,y,z) = \sum_{-\infty}^{\infty} \mathbf{E}_n(x,y)\epsilon^{-j\beta_n z} \tag{8.7-16}$$

The quantities $\mathbf{E}_n(x,y)\epsilon^{-j\beta_n z}$ are known as space harmonics by analogy with time-domain Fourier series. Now we can impose the necessary condition that our solution should satisfy the wave equation, Equation (8.1-26). Substituting Equation (8.7-16) into the wave equation, we obtain

$$\nabla^2\left[\sum_{-\infty}^{\infty} \mathbf{E}_n(x,y)\epsilon^{-j\beta_n z}\right] + k^2\left[\sum_{-\infty}^{\infty} \mathbf{E}_n(x,y)\epsilon^{-j\beta_n z}\right] = 0 \tag{8.7-17}$$

Since the wave equation is linear, we can interchange the order of differentiation and summation, obtaining

$$\sum_{-\infty}^{\infty} [\nabla^2\mathbf{E}_n(x,y)\epsilon^{-j\beta_n z} + k^2\mathbf{E}_n(x,y)\epsilon^{-j\beta_n z}] = 0 \tag{8.7-18}$$

From this equation we see that if each space harmonic is itself a solution of the wave equation, that is, if the bracketed term is zero for each value of n, the summation of space harmonics automatically satisfies the wave equation, Equation (8.7-17). Thus each space harmonic is chosen as a solution of the wave equation and consequently must also satisfy Maxwell's Equations. These statements do not imply that each space harmonic satisfies all of the boundary conditions in the structure; only the complete solution, Equation (8.7-16), satisfies this requirement. *Physically, this means that it is impossible to have wave propagation in a periodic structure consisting solely of one space harmonic; a mode of propagation must necessarily consist of an infinite number of space harmonics.*

For simplicity in this section we have considered a periodic structure of infinite length. As in the case of ordinary transmission lines, a finite length structure will have propagation properties identical to those of the infinite structure, except that forward and backward traveling waves must be superimposed to allow for mismatches at the ends of the structure. In nearly all tubes using periodic structures, the structure is matched at both ends so as to eliminate reflected waves.

(*b*) *Field Solutions in a Particular Slow-Wave Structure*

A simple example may help to clarify some of the above points. Let us investigate wave propagation in the periodic structure shown in Figure 8.7-4.[11] This structure consists of two parallel infinite conducting planes.

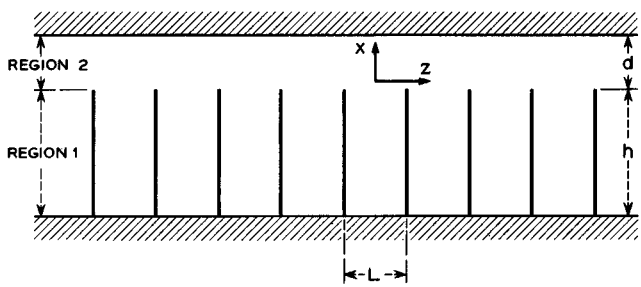

FIG. 8.7-4 A slow-wave structure consisting of thin fins mounted perpendicular to one plate of a parallel-plate line. The direction of propagation is to the right or left.

On the bottom plane are mounted infinitesimally thin conducting fins of height h and infinite width (in the direction perpendicular to the page). The separation from the top of the fins to the top plane is d.

[11]Reference 8g.

A set of coordinate axes may be chosen as shown, with the origin at the center between two fins. The periodic spacing is L. Slow-wave propagation can exist in the z direction.

As in any microwave structure there are many modes of propagation possible. The mode of lowest frequency is often the simplest to analyze, and in most structures it is the most commonly used mode. We shall thus content ourselves with studying the simplest mode of the structure shown in Figure 8.7-4. Since the structure itself is invariant in the y direction, we shall assume the electromagnetic fields are also invariant in this direction. A consequence of this assumption is that spatial derivatives in the y direction must be zero.

It will be convenient to divide the space between the planes into two regions. Region 1 is the space for which $-h \leq x \leq 0$, the region of the vanes. Region 2 is the gap above the vanes for which $0 \leq x \leq d$. We can then solve Maxwell's Equations separately in the two regions, and finally, we can equate the tangential components of electric and magnetic field at the boundary between the two regions, that is, at $x = 0$. Continuity of the tangential electric and magnetic field vectors is necessary, as discussed in Section 8.3. In each region we shall choose our solutions so that the boundary condition at a perfect conductor of zero tangential electric field is satisfied.

Region 1 will be considered first. Consider the unit cell bounded by the two vanes at $z = \pm L/2$. The simplest solution here is a standing-wave solution to Maxwell's Equations consisting of E_z and H_y components only. The desired solution for E_z is

$$E_z = A \sin k(x + h) \tag{8.7-19}$$

where A is an arbitrary constant and $k = \omega/c$. It may be verified that this solution satsifies the wave equation, Equation (8.1-26), and the boundary condition $E_z = 0$ at $x = -h$. The solution for the magnetic field may be obtained from Equation (8.7-19) by use of the second of Equations (8.1-18),

$$j\omega\mu_o H_y = \frac{\partial E_z}{\partial x} - \frac{\partial E_x}{\partial z} \tag{8.7-20}$$

Using Equation (8.7-19) and the fact that E_x is zero, we obtain

$$H_y = -j\sqrt{\frac{\varepsilon_o}{\mu_o}} A \cos k(x + h) \tag{8.7-21}$$

It may be verified that the other components of **H** are zero.

Floquet's Theorem, Equation (8.7-7), may be used to find the fields in region 1 in between the other pairs of vanes. If the gaps are numbered in

order with $N = 0$ corresponding to the gap centered at $z = 0$, $N = 1$ to the gap centered at $z = L$, etc., we then have from Floquet's Theorem, in all of region 1,

$$E_z = A \sin k(x + h)\, \epsilon^{-jN\beta_o L} \tag{8.7-22}$$

$$H_y = -j\sqrt{\frac{\varepsilon_o}{\mu_o}} A \cos k(x + h)\, \epsilon^{-jN\beta_o L} \tag{8.7-23}$$

Next, we proceed to solve Maxwell's Equations in region 2. The general solution is given by Equation (8.7-16). Let us consider the z component:

$$E_z = \sum_{-\infty}^{\infty} E_{zn}(x)\epsilon^{-j\beta_n z} \tag{8.7-24}$$

Each space harmonic will satisfy Maxwell's Equations, or equivalently, the wave equation, Equation (8.1-26), which in our case can be written

$$\left(\frac{\partial^2}{\partial x^2} + \frac{\partial^2}{\partial z^2} + k^2\right) E_{zn}(x)\epsilon^{-j\beta_n z} = 0 \tag{8.7-25}$$

Performing the z differentiation, we obtain

$$\left(\frac{\partial^2}{\partial x^2} - \beta_n{}^2 + k^2\right) E_{zn}(x)\epsilon^{-j\beta_n z} = 0 \tag{8.7-26}$$

or simply

$$\left(\frac{\partial^2}{\partial x^2} - \beta_n{}^2 + k^2\right) E_{zn} = 0 \tag{8.7-27}$$

This equation has the solution

$$E_{zn} = B_n \sinh \gamma_n(x - C_n) \tag{8.7-28}$$

where

$$\gamma_n{}^2 \equiv \beta_n{}^2 - k^2$$

and B_n and C_n are arbitrary constants. The hyperbolic sine solution rather than the trigonometric sine solution has been chosen so that $\beta_n{}^2 > k^2$, since we are looking for slow waves. Since the phase velocity for a space harmonic according to Equation (8.7-24) is given by

$$v_{pn} = \frac{\omega}{\beta_n} \tag{8.7-29}$$

we see that $v_{pn} < c$ if $\beta_n > k = \omega/c$.

Equation (8.7-24) may now be written using Equation (8.7-28):

$$E_z = \sum_{-\infty}^{\infty} B_n \sinh \gamma_n(x - C_n)\, \epsilon^{-j\beta_n z} \tag{8.7-30}$$

The boundary condition that $E_z = 0$ at $x = d$ can be satisfied if we choose

$$C_n = d \tag{8.7-31}$$

so that

$$E_z = \sum_{-\infty}^{\infty} B_n \sinh \gamma_n(x - d)\, \epsilon^{-j\beta_n z} \tag{8.7-32}$$

Next we equate the two expressions for E_z given by Equations (8.7-22) and (8.7-32) at the boundary between regions 1 and 2. We can simplify this matching technique somewhat by noting that Floquet's Theorem implies that if solutions are matched at the boundary in one cell of a periodic structure, they will be matched in all cells. Let us therefore match over the range $-L/2 \leq z \leq L/2$. We obtain

$$-\sum_{-\infty}^{\infty} B_n \sinh \gamma_n d\, \epsilon^{-j\beta_n z} = A \sin kh$$

for

$$-\frac{L}{2} \leq z \leq \frac{L}{2} \tag{8.7-33}$$

The coefficients B_n can be obtained by the following process. Multiply both sides of the equation by $\epsilon^{+j\beta_m z}$ and integrate over a period:

$$-\sum_{-\infty}^{\infty} B_n \sinh \gamma_n d \int_{-L/2}^{L/2} \epsilon^{j(\beta_m - \beta_n)z} dz = A \sin kh \int_{-L/2}^{L/2} \epsilon^{j\beta_m z} dz \tag{8.7-34}$$

The right-hand side is easily integrated. The left-hand side can be manipulated as follows, using Equation (8.7-15):

$$\int_{-L/2}^{L/2} \epsilon^{j(\beta_m - \beta_n)z} dz = \int_{-L/2}^{L/2} \epsilon^{j(2\pi/L)(m-n)z} dz = \begin{cases} 0 \text{ for } n \neq m \\ L \text{ for } n = m \end{cases} \tag{8.7-35}$$

Equation (8.7-34) thus becomes

$$-B_m L \sinh \gamma_m d = A \frac{\sin \dfrac{\beta_m L}{2}}{\dfrac{\beta_m}{2}} \sin kh \tag{8.7-36}$$

By substituting Equation (8.7-36) into Equation (8.7-32), we obtain for E_z in region 2

$$E_z = -A \sin kh \sum_{-\infty}^{\infty} \frac{\sin \dfrac{\beta_n L}{2}}{\dfrac{\beta_n L}{2}} \frac{\sinh \gamma_n(x - d)}{\sinh \gamma_n d} \epsilon^{-j\beta_n z} \tag{8.7-37}$$

We thus have a complete description of the z component of electric field in terms of an arbitrary amplitude factor A.

The other components of the electric and magnetic fields in region 2 may be obtained as follows. First, because $E_y = 0$ in region 1, it will also be zero in region 2, since tangential components of **E** are continuous at the boundary.

Next, the divergence equation, Equation (8.1-16), of Maxwell's Equations is written (using Equation (2) of Appendix XII) as

$$\frac{\partial E_x}{\partial x} + \frac{\partial E_z}{\partial z} = 0 \tag{8.7-38}$$

since there is no free charge in the region. This equation can be solved for E_x:

$$E_x = -\int \frac{\partial E_z}{\partial z} \partial x \tag{8.7-39}$$

Performing the indicated operations on Equation (8.7-37), we obtain

$$E_x = -jA \sin kh \sum_{-\infty}^{\infty} \frac{\sin \frac{\beta_n L}{2}}{\frac{\gamma_n L}{2}} \frac{\cosh \gamma_n (x - d)}{\sinh \gamma_n d} \epsilon^{-j\beta_n z} \tag{8.7-40}$$

The components of the magnetic field can be obtained by use of Equations (8.1-18). Since $E_y = 0$, and derivatives with respect to y are also zero, we see that

$$H_x = H_z = 0 \tag{8.7-41}$$

Equations (8.7-37), (8.7-40), and (8.1-18) together give, after simplification,

$$H_y = -j\omega\varepsilon_o A \sin kh \sum_{-\infty}^{\infty} \frac{\sin \frac{\beta_n L}{2}}{\frac{\gamma_n \beta_n L}{2}} \frac{\cosh \gamma_n (x - d)}{\sinh \gamma_n d} \epsilon^{-j\beta_n z} \tag{8.7-42}$$

At this point we have a complete description of the fields in the slow-wave structure, assuming that we know what value of β_o corresponds to a given frequency of operation. All the values of β_n and γ_n can be obtained from β_o using Equation (8.7-15) and the relation defining γ_n,

$$\gamma_n^2 = \beta_n^2 - k^2 \tag{8.7-43}$$

A sketch of the electric field lines for $\beta_o L = \pi/10$ is shown in Figure 8.7-5.

An equation determining β_o from the frequency may be obtained by matching the tangential components of the magnetic field at the boundary between regions 1 and 2. However, at this point we must note that the

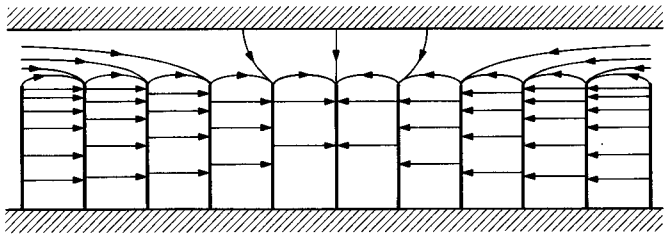

FIG. 8.7-5 Electric field lines in the slow-wave structure of Figure 8.7-4 for $\beta_o L = \pi/10$.

solutions we have obtained are only approximate, due to the neglect of fringing fields near the vane tips in region 1. Because of this approximation, the magnetic fields in the two regions will not match point for point at the boundary. Let us therefore content ourselves with matching at the mid-point of the gap, where $z = 0$.

Equating Equations (8.7-21) and (8.7-42) for $z = 0$ and $x = 0$, we obtain

$$\frac{\cot kh}{kh} = \sum_{-\infty}^{\infty} \frac{\sin \frac{\beta_n L}{2}}{\frac{\beta_n L}{2}} \frac{\coth \gamma_n d}{\gamma_n h} \tag{8.7-44}$$

where

$$k = \omega\sqrt{\mu_o \varepsilon_o}$$

$$\beta_n = \beta_o + \frac{2\pi n}{L}$$

$$\gamma_n = \sqrt{\beta_n^2 - k^2}$$

The solutions to this equation are obtained numerically. We shall discuss the resultant ω-β diagram in the next section.

Let us review briefly what we have accomplished in this section. We have used approximate solutions to Maxwell's Equations in a periodic structure to obtain the slow-wave propagation fields. One may wonder as to the effect of the approximations involved. It turns out that the resultant ω-β diagram is relatively insensitive to small errors in the shapes of the field solutions, so that information derived from the ω-β diagram can be taken to be quite accurate. The exact shape of the fields will be somewhat in error, but this information is usually needed only approximately.

(c) *The Brillouin Diagram*

We have seen in Sections (a) and (b) that the electric or magnetic field for a propagating mode in a slow-wave structure can be expanded as a

summation of space harmonics, as in Equation (8.7-16), which we repeat here.

$$\mathbf{E}(x,y,z) = \sum_{-\infty}^{\infty} \mathbf{E}_n(x,y)\epsilon^{-j\beta_n z} \tag{8.7-45}$$

where

$$\beta_n = \beta_o + \frac{2\pi n}{L} \tag{8.7-46}$$

Each space harmonic propagates in the positive z direction with a different phase velocity given by

$$v_{pn} = \frac{\omega}{\beta_n} \tag{8.7-47}$$

Therefore, the mode of propagation cannot be characterized at some frequency by a unique velocity as it was in the case of ordinary smooth waveguides. Referring to our previous interpretation of the phase velocity, we see that *it is no longer possible for an "observer" to move so as to be always in the same phase of the total field. It is possible for the "observer" to move in synchronism with only one of the space harmonics that make up the total field.* The phases of the other space harmonics will be continually changing as viewed by the "observer." If the "observer" takes a time average of the total field that he sees over a sufficiently long period of time as he moves in synchronism with one of the space harmonics, the average obtained will be that given by the synchronous space harmonic alone, the net contribution of the others being negligible in comparison. It will be useful in later chapters to bear in mind this interpretation of the phase velocity.

Let us now plot the ω-β curve for the periodic structure of Figure 8.7-4. We will want to make sure we include values of the propagation constant β_n for all of the space harmonics. This ω-β diagram is known as a Brillouin diagram.[12] It is customary to label the abscissa as the β axis instead of the β_n axis. Each branch of the Brillouin diagram is numbered according to the space harmonic to which it refers.

The fundamental space harmonic ($n = 0$) propagation constant is obtained as a function of frequency from Equation (8.7-44). Since this is a transcendental equation, there will be an infinite number of frequencies or modes of propagation for each value of β. This infinite number of modes should come as no surprise, since we first encountered them in the analysis of ordinary waveguides. The ω-β curves for the fundamental space harmonics are shown in Figure 8.7-6, including the higher-order modes. We have

[12]After L. Brillouin who studied extensively wave propagation in periodic structures. See Reference 8f.

included only the modes propagating in the positive z direction for the time being. The negative propagating modes have branches which are the mirror images of these about the ω axis, as in Figure 8.5-4. We have labeled the lower branch with a zero, indicating that it corresponds to the fundamental ($n = 0$) space harmonic. We shall omit labeling the higher-order modes. Physically, these higher modes correspond approximately to additional half wavelengths in region 1 of Figure 8.7-4.

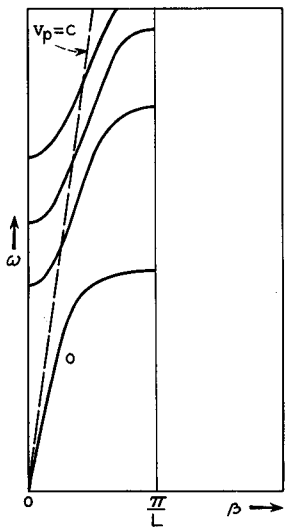

FIG. 8.7-6 The branches of the Brillouin diagram corresponding to the fundamental space harmonics of modes propagating in the positive z direction.

Now from Equation (8.7-46), we see that the Brillouin diagram branches for the other space harmonics are obtained by taking the fundamental space harmonic branches in Figure 8.7-6 and translating them parallel to the β axis through distances which are integral multiples of $2\pi/L$. Figure 8.7-7 shows this construction utilized to obtain the plus-one and minus-one space harmonics.

It would be enlightening at this point to consider the group velocity in a periodic structure. It is defined as in Section 8.5 for ordinary waveguides (Equation (8.5-27)):

$$v_g = \frac{\partial \omega}{\partial \beta} \tag{8.7-48}$$

It has the same physical significance as before; that is, it is the velocity at which energy is transported down the periodic structure. Since all of the space harmonics must be taken together to constitute a mode of propagation, we would expect all of them to have the same group velocity, corresponding to the velocity of energy transport. A glance at Figure 8.7-7 shows that this is indeed the case. All of the branches for any mode of propagation have the same slope at any given frequency, hence, the same group velocity. Group and phase velocities are measured by geometrical constructions as in Figure 8.5-2. It should be noted that no equation similar to Equation (8.5-28) exists for slow-wave structures.

Figure 8.7-7 also shows that the minus space harmonics ($n = -1$, -2, etc.) have phase velocities that are negative, albeit the group veloc-

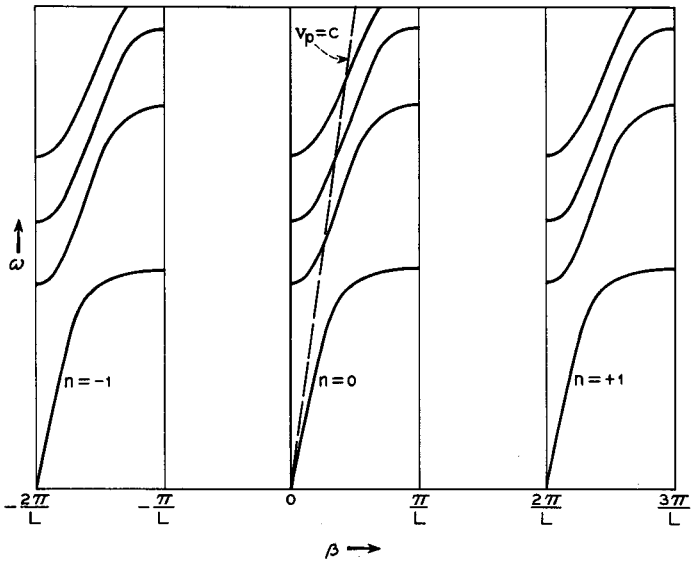

FIG. 8.7-7 Branches of the Brillouin diagram for the three lowest space harmonics of modes propagating in the positive z direction.

ity is positive. This is an interesting property of periodic structures which has no parallel in the smooth waveguide case. This means that an electron "observer" can remain in synchronism with a wave which is actually transporting energy in the opposite direction. This remarkable property has made possible the backward-wave oscillator and M-Carcinotron which will be described in later chapters.

Because the slow-wave structure shown in Figure 8.7-4 consists of two separate conducting members, it has no lower cutoff frequency, and in fact it propagates signals with frequencies ranging down to zero frequency, as is evident from the Brillouin diagram.

The branches marked $n = -1$, 0, and $+1$ in Figure 8.7-7 correspond to the principal mode of propagation. The broken lines in the figure have slopes corresponding to phase velocities of $+c$ and $-c$, where c is the velocity of light. We see that all spatial harmonics of the principal mode of propagation lie either to the right or to the left of the $v_p = \pm c$ lines rather than between these lines. This means that the phase velocities of the fundamental and higher-order space harmonics of the principal mode are of magnitude less than the velocity of light. Furthermore, the phase velocity of the $n = 1$ space harmonic of the principal mode is less than that of the fundamental, or $n = 0$ space harmonic, and the phase velocity of the $n = 2$ space harmonic is less than that of the $n = 1$ space harmonic.

So far we have considered energy propagating solely in the positive z direction. The branches for the negative propagating modes are obtained by simply reflecting all the branches of Figure 8.7-7 about the ω axis, as in Figure 8.7-8, where the complete Brillouin diagram is shown. It is seen that

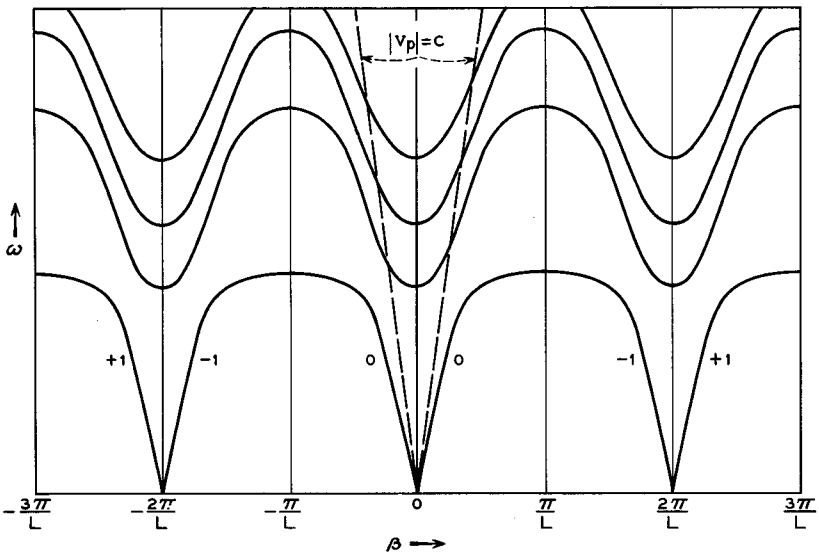

FIG. 8.7-8 Complete Brillouin diagram for the periodic structure of Figure 8.7-4.

all of these additional branches have negative group velocities, as expected. The numbers of these additional branches are chosen so as to correspond to the reflected branches.

(*d*) *Power Flow*

In order to complete our discussion of periodic structures we must consider a means of calculating power flow from a knowledge of the electromagnetic fields of a propagating mode.

Equation (8.5-26) states that the power flow in a smooth waveguide is given by the product of the group velocity and the energy stored per unit length.[13] Now, for a lossless periodic structure Floquet's Theorem, Equation (8.7-7), states that the fields in all cells are equal in magnitude, differing only in phase. This means that the stored energy in each unit cell

[13]In cases where the electromagnetic fields are known only approximately, this gives a more accurate evaluation of the power flow than does integration of the Poynting vector.

of the periodic structure is the same as that in all the others. Hence, the stored energy per unit length can be simply calculated by taking the stored energy in any one unit cell and dividing by the length of the cell. With this adaptation, Equation (8.5-26) can be used to calculate the power flow in a periodic structure. It may be written as

$$P = v_g \frac{W_L}{L} \tag{8.7-49}$$

where W_L is the time average energy stored per cell and L is the length of the cell.

In calculating the average stored energy per period, it is convenient to realize that the time average stored electric energy per period is equal to the time average stored magnetic energy. Thus it is necessary to calculate only the average stored energy due to either the magnetic or electric fields and multiply this by two. This relationship can be proved rigorously for a periodic structure, but the proof is rather long and complicated.[14]

As an example, we may compute the power flow per unit width in the periodic structure of Figure 8.7-4. We have already solved for the field components, finding expressions for E_z and H_y in region 1 and E_x, E_z, and H_y in region 2, the other components being zero. In finding the stored energy it will be easier to use the magnetic field expressions, since only one component is involved.

The time average stored energy per cell (see Appendix XIV) is given by

$$W_L = \frac{\mu_o}{2} \int_{\text{unit cell}} |\mathbf{H}|^2 dv \tag{8.7-50}$$

Since the structure is of infinite width, we shall determine only the power flow per unit width, designated

$$W_{Lw} = \frac{\mu_o}{2} \int\int_{\text{unit cell}} |H_y|^2 dz dx \tag{8.7-51}$$

where use is made of the fact that $H_x = H_z = 0$.

The contribution to this integral in region 1 is obtained by using Equation (8.7-21):

$$\begin{aligned} W_{Lw1} &= \frac{1}{2}\varepsilon_o L A^2 \int_{-h}^{0} \cos^2 k(x+h) dx \\ &= \frac{1}{4}\varepsilon_o L h A^2 \left[1 + \frac{\sin 2kh}{2kh}\right] \end{aligned} \tag{8.7-52}$$

[14]Reference 8g, pp. 10–14.

In region 2, H_y is given by Equation (8.7-42), repeated below:

$$H_y = -j\omega\varepsilon_o A \sin kh \sum_{-\infty}^{\infty} \frac{\sin \frac{\beta_n L}{2}}{\frac{\gamma_n \beta_n L}{2}} \frac{\cosh \gamma_n (x - d)}{\sinh \gamma_n d} \epsilon^{-j\beta_n z} \tag{8.7-53}$$

$| H_y |^2$ is obtained by multiplying this quantity by its conjugate,

$$H_y^* = +j\omega\varepsilon_o A \sin kh \sum_{-\infty}^{\infty} \frac{\sin \frac{\beta_m L}{2}}{\frac{\gamma_m \beta_m L}{2}} \frac{\cosh \gamma_m (x - d)}{\sinh \gamma_m d} \epsilon^{+j\beta_m z} \tag{8.7-54}$$

Equation (8.7-51) becomes, for region 2,

$$W_{Lw2} = \tfrac{1}{2}\mu_o \omega^2 \varepsilon_o^2 A^2 \sin^2 kh \sum_m \sum_n \int_0^d \int_{-L/2}^{L/2} C_m C_n \epsilon^{j(2\pi/L)(m-n)z} dz dx \tag{8.7-55}$$

where we have written

$$C_n = \frac{\sin \frac{\beta_n L}{2}}{\frac{\gamma_n \beta_n L}{2}} \frac{\cosh \gamma_n (x - d)}{\sinh \gamma_n d}$$

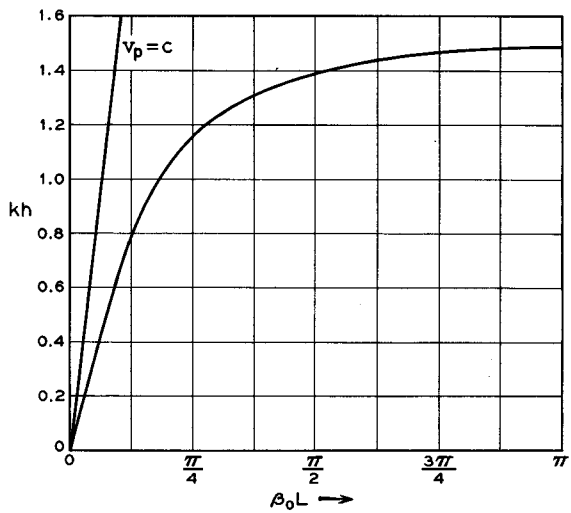

FIG. 8.7-9 Fundamental branch of the Brillouin diagram for the slow-wave structure of Figure 8.7-4, with dimensions given by $h/d = 4$ and $h/L = 5$.

Performing the z integration, using Equation (8.7-35), we obtain

$$W_{Lw2} = \frac{1}{2}\mu_o\omega^2\varepsilon_o{}^2A^2L\sin^2 kh \sum_{-\infty}^{\infty} \frac{\sin^2\frac{\beta_nL}{2}}{\gamma_n{}^2\left(\frac{\beta_nL}{2}\right)^2}\int_0^d \frac{\cosh^2\gamma_n(x-d)}{\sinh^2\gamma_nd}dx \tag{8.7-56}$$

Integrating this expression and simplifying, we obtain

$$W_{Lw2} = \frac{1}{4}\varepsilon_oLdA^2\sin^2 kh \sum_{-\infty}^{\infty} \frac{k^2}{\gamma_n{}^2}\left(\frac{\sin\frac{\beta_nL}{2}}{\frac{\beta_nL}{2}}\right)^2 1 + \frac{\sinh 2\gamma_nd}{2\gamma_nd} \tag{8.7-57}$$

The total time average stored energy is the sum of that given by Equations (8.7-52) and (8.7-57). Although Equation (8.7-57) is complicated, it is easily evaluated, since the series converges quite rapidly.

Next, we can compute the power flow, using Equation (8.7-49) for a particular geometry of the finned structure shown in Figure 8.7-4. Consider a structure with dimensions chosen such that $h/d = 4$ and $h/L = 5$. Equa-

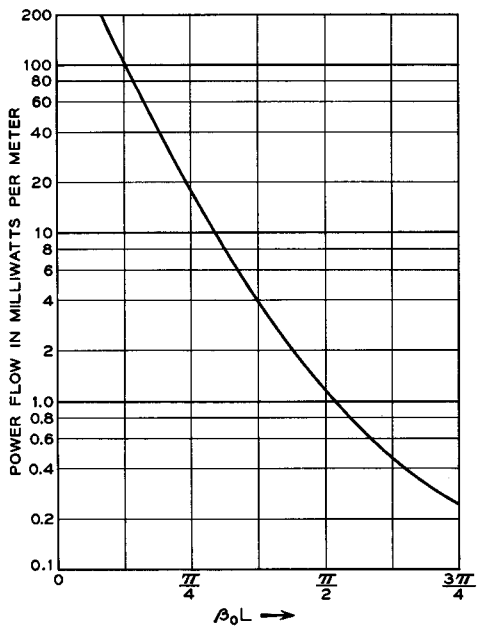

FIG. 8.7-10 Power per unit width in the structure of Figure 8.7-4 for a vane tip-to-tip voltage of one volt. $h/d = 4$ and $h/L = 5$.

tion (8.7-44) is solved numerically to obtain the fundamental space harmonic branch of the Brillouin diagram for the lowest frequency mode. This is shown in Figure 8.7-9. A line with slope equal to the velocity of light is drawn in for reference. We note, as before, that the phase velocity at every point on the curve is less than the velocity of light. The upper cutoff frequency is approximately that for which the vanes are a quarter wavelength long. We might have expected this, since the input impedance to a quarter wavelength shorted line is infinite, presenting an open circuit as far as axial current flow is concerned.

Having thus determined the relationship between ω and β_o, we can proceed to calculate the power flow. It will be more interesting here to deal with an actual structure, designed for a specific operating frequency. Let us choose dimensions such that the mode cuts off at 10 Gc. This occurs for

$$h = 0.706 \text{ cm}$$
$$L = 0.141 \text{ cm} = h/5$$
$$d = 0.1766 \text{ cm} = h/4$$

The power flow per unit width of the structure is presented in Figure 8.7-10 as a function of $\beta_o L$. This curve is obtained by multiplying the group velocity by the time average stored energy per unit length, where the former quantity is obtained by measuring slopes in Figure 8.7-9. The power flow given is that amount required to produce a peak voltage of one volt from one vane tip to the next. From Equation (8.7-19) we see that this occurs for

$$E_z(0)L = AL \sin kh = 1 \text{ volt}$$

The power flow goes to zero as βL approaches π because the group velocity goes to zero. On the other hand, as βL goes to zero, we approach the dc condition where the top plate is all at one potential and the fins are all at the opposite potential. It becomes more and more difficult to maintain a voltage difference of one volt from one vane to the next, and the power required becomes infinitely large.

PROBLEMS

8.1 The equivalent circuit for the cavity in Figure 8-2 is given by a resistance, capacitance, and inductance in parallel. (a) Calculate the values of the capacitance and inductance at 3000 Mc for the dimensions given in the text. (b) The magnetic field in the inductive sections of the cavity can be written

$$H_\theta = \frac{I}{2\pi r} \frac{\cos \frac{\omega}{c} z}{\cos \frac{\omega}{c} l}$$

where z is measured from the top or bottom wall, respectively, and I is the current through the equivalent circuit inductance. Using Equation (8.4-19), find an expression for the ohmic power loss in the cavity at resonance for the dimensions given in the text. From this power loss find an expression for the resistance in the equivalent circuit. Neglect losses in the capacitive region of the cavity.

8.2 Scaling laws apply exactly to microwave structures whose walls are perfect conductors and approximately to others. The scaling law may be stated mathematically as follows. If $\mathbf{E}(x,y,z,\omega t)$ is a solution to the wave equation, then $\mathbf{E}(Kx,Ky,Kz, K\omega t)$ is also a solution, where K is a numerical constant. Demonstrate the validity of this statement.

8.3 Suppose that the cavity of Problem 8.1 is scaled to be resonant at K times 3000 Mc. (a) What are the resistance, capacitance, and inductance of the equivalent circuit for the new cavity, assuming the cavity walls are made of the same material? (b) What is the ratio of the Q's of the two circuits, where $Q = R/\omega L$.

8.4 By applying Stoke's theorem to Equation (8.1-14) show that the component of magnetic field perpendicular to a perfect conductor is zero, given that the parallel component of electric field is zero.

8.5 Show that the resistive power loss in a conductor may be derived assuming a uniform current density in a wall of a thickness equal to the skin depth, where the wall current per unit width is given by

$$I_z = \int_0^\infty J_z dx$$

and J_z is given by Equation (8.4-13).

8.6 Slow-wave structures may sometimes be represented by an equivalent circuit consisting of a uniform lossless transmission line periodically loaded by either a series or a shunt reactance. If $Z_o = 1/Y_o$ is the characteristic impedance and φ_o is the phase shift per period of the unloaded line, then periodic shunt loading due to a susceptance B results in the relation

$$\cos \beta_o L = \cos \varphi_o - \frac{B}{2Y_o} \sin \varphi_o$$

where $\beta_o L$ is the periodic phase shift of the periodically loaded structure. Similarly, for periodic series loading due to a reactance X, one obtains

$$\cos \beta_o L = \cos \varphi_o - \frac{X}{2Z_o} \sin \varphi_o$$

Prove either one of these relationships using the fact that corresponding voltages and currents in adjacent cells are related by the factor $\epsilon^{-j\beta_o L}$. Use the results of uniform transmission line theory which state that the input and output voltages and currents for a line of electrical length φ_o are related by:

$$V_{\text{in}} = V_{\text{out}} \cos \varphi_o + jI_{\text{out}} Z_o \sin \varphi_o$$

$$I_{\text{in}} = I_{\text{out}} \cos \varphi_o + jV_{\text{out}} Y_o \sin \varphi_o$$

8.7 How is Equation (8.7-37) modified if the vanes of Figure 8.7-4 have a finite thickness Δ?

8.8 From Equation (8.7-37) compute the relative magnitudes of the $n = 0, \pm 1, \pm 2$ space harmonics at the frequency for which $\beta_o L = \pi/2$. Compute them at the value of x for which they are a maximum.

8.9 A slow-wave structure has an equivalent circuit consisting of a cascade of filter sections whose shunt arm is a pure capacitance C and whose series arm is an open-circuited transmission line. The transmission line has a characteristic admittance of $\frac{1}{2}\omega_o C$, where ω_o is the lowest radian resonant frequency of the line; i.e., the susceptance of the series arm is given by $B_1 = \frac{1}{2}\omega_o C \tan(\pi\omega/2\omega_o)$. Sketch the Brillouin diagram over the range $0 \leq \omega \leq 4\omega_o$ and $-2\pi \leq \beta L \leq 2\pi$. Determine the cutoff frequencies accurately and then qualitatively sketch in the curves. Make use of the filter formula $\cos \beta_o L = 1 + B_2/2B_1$, where B_2 is the susceptance of the shunt arm.

8.10 By studying the symmetries of a slow-wave structure one may deduce certain facts about its space harmonics. In the figure is shown an interdigital line, assumed to be infinitesimally thin in the y direction. This structure has a symmetry such that a translation of $L/2$ in the z direction accompanied by a reflection about the y-z plane results in the structure mapping back onto itself.

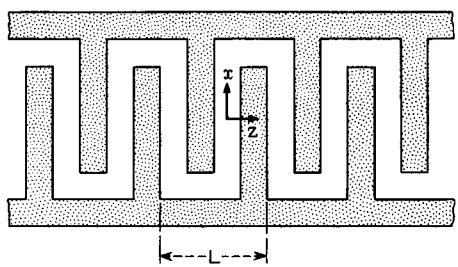

Problem 8.10

The solution for the electric field near $x = 0$ is of the form

$$E_z = \sum_{-\infty}^{\infty} (A_n \cos kx + B_n \sin kx)\epsilon^{-|\gamma_{ny}|}\epsilon^{-j\beta_n z}$$

Because of the symmetry described above we can replace z by $z + (L/2)$ and x by $-x$, and the resulting expression for E_z can differ from the original only by a complex constant. Use these facts to show that either $A_n = 0$ for n odd and $B_n = 0$ for n even (symmetric mode), or else $A_n = 0$ for n even and $B_n = 0$ for n odd (antisymmetric mode).

REFERENCES

Four general references on electromagnetic field theory and its application to waveguides and cavities are:

8a. S. Ramo and J. R. Whinnery, *Fields and Waves in Modern Radio*, John Wiley and Sons, Inc., New York, 1959.

8b. C. G. Montgomery, R. H. Dicke, and E. M. Purcell, "Principles of Microwave Circuits," *MIT Radiation Laboratory Series*, Vol. 8, McGraw-Hill Book Co., Inc., New York, 1948.
8c. J. A. Stratton, *Electromagnetic Theory*, McGraw-Hill Book Co., Inc., New York, 1941.
8d. H. H. Skilling, *Fundamentals of Electric Waves*, John Wiley and Sons, Inc., New York, 1948.
8e. G. C. Southworth, *Principles and Applications of Waveguide Transmission*, D. Van Nostrand Co., Inc., Princeton, N. J., 1950.

The following references contain material on slow-wave structures:

8f. L. Brillouin, *Wave Propagation in Periodic Structures*, Dover Publications, Inc., New York, 1953.
8g. D. A. Watkins, *Topics in Electromagnetic Theory*, Chapter 1, John Wiley and Sons, Inc., New York, 1958.
8h. J. R. Pierce, *Traveling-Wave Tubes*, D. Van Nostrand Co., Inc., Princeton, N. J. 1950.
8i. J. C. Slater, *Microwave Electronics*, Chapter 8, D. Van Nostrand Co., Inc., Princeton, N. J., 1950.
8j. A. H. W. Beck, *Space-Charge Waves and Slow Electromagnetic Waves*, Chapter 3, Pergamon Press, Inc., New York, 1958.
8k. E. Belohoubek, "Propagation Characteristic of Slow-Wave Structures Derived from Coupled Resonators," *RCA Review* **19**, 283-310, June, 1958.

Other references covering specific items discussed in the chapter are:

8.1 K. Fujisawa, "General Treatment of Klystron Resonant Cavities," *Trans. IRE*, **MTT-6**, no. 4, 344–358, October, 1958.
8.2 H. H. Skilling, *Electric Transmission Lines*, McGraw-Hill Book Co., Inc., New York, 1951.
8.3 R. B. Adler, "Properties of Guided Waves on Inhomogeneous Cylindrical Structures," *RLE Tech. Report No.* 102 (MIT), 1949.
8.4 W. W. Hansen, "A Type of Electrical Resonator," *J. Appl. Phys.* **9**, 654–663, October, 1938.